EFFECT OF COOLING RATE AND MODIFICATION ON THE MICROSTRUCTURE AND TENSILE PROPERTIES OF Al-Si-Mg ALLOY

BY

EGOLE, CHIJIOKE PETER (B.ENG.)

20114771908

A THESIS SUBMITTED TO THE POSTGRADUATE SCHOOL

FEDERAL UNIVERSITY OF TECHNOLOGY, OWERRI

IN PARTIAL FULFILLMENT OF THE REQUIREMENT FOR THE AWARD OF THE DEGREE OF MASTERS OF ENGINEERING (M.ENG) IN MATERIALS AND METALLURGICAL ENGINEERING (METALLURGICAL ENGINEERING)

MARCH, 2014.

CERTIFICATION

I certify that this research work "Effect of Cooling Rate and Modification on the Microstructure and Tensile Properties of Al-Si-Mg Alloy," was carried out by me, **Egole Chijioke Peter 20114771908** in partial fulfilment for award of Masters Degree (M.ENG) in Materials and Metallurgical Engineering, Federal University of Technology, Owerri.

---------- ----------

Engr. Prof. O.E Okorafor Date
(Supervisor)

---------- ----------

Dr. C.S Nwobodo Date
(HOD MME)

---------- ----------

Engr. Prof. E.E. Anyanwu Date
(Dean SEET)

---------- ----------

Engr. Prof. (Mrs.) K.B. Oyoh Date
(Dean, Postgraduate School)

---------- ----------

External Examiner Date

DEDICATION

This research work is dedicated to the Almighty God.

ACKNOWLEDGEMENT

I express my unreserved gratitude and appreciation to my project supervisor, Engr. Prof. O.E Okorafor for the time he put into this research work. All his efforts, support and advice during and after the experiments made this work a reality.

I also thank my lecturers, Engr. Prof. O.O. Onyemaobi, Engr. Prof. J.E.O Ovri, Dr. C.S. Nwobodo (HOD), Prof. C.N. Anyakwo (Associate Dean SEET), Dr. R.I Ejimofor, Prof. E.E. Nnuka and Dr. N.E. Ideyi who undertook our postgraduate courses.

I will not fail to appreciate Engr. U. Mark, Engr. A.I. Ogbonna, Engr. U.S Ikele, Engr. P.C. Agu and Mr. C. Ugwuegbu for their advice at one point or the other. I also thank my colleagues in the program, especially Mr. Anaele Justus U., for their collective contributions towards the success of our program.

My heartfelt appreciation also goes to my lovely parents Mr. and Mrs. J.R.O Egole (ESQ) for their support and prayers through the time of my program.

Engr. Prof. E.E. Anyawu (Dean SEET) and Engr. Prof. (Mrs.) K.B Oyoh (Dean Postgraduate School) are wonderfully appreciated in this work.

ABSTRACT

The effect of cooling rate and modification on the microstructure and tensile properties of Al-Si-Mg alloys was carried out. Castings were produced using a stepped pattern that has different section thicknesses. Sand casting technique was used. A thermocouple inserted into the mould cavity recorded the cooling rates for the different sections. The Al5.43%Si3.83%Mg which was melted in the crucible furnace was modified with sodium (Na) and strontium (Sr) in separate cases. The molten metal was poured at 750^{o}C and allowed to cool and to solidify in the mould. Tensile tests, hardness test and microstructural analyses were carried out using standard specifications and methods. The tensile test results showed that the component with minimum section thickness (5mm) had the highest cooling rate and gave the highest tensile strength of 110N/mm^{2}. It was also revealed from the hardness test results that the section with minimum thickness (5mm) had the highest hardness of 46.5 HRB. From the photomicrographs produced, the 5mm thick section with the fastest cooling rate showed finer grains than the other sections, with the thickest section of 40mm showing the most coarse microstructure at slowest cooling rate. Also structures modified with sodium and strontium displayed better microstructural and tensile properties when compared with the unmodified structures. Modification effect is better with sodium than strontium.

TABLE OF CONTENTS

CHAPTER THREE

LIST OF TABLES

LIST OF FIGURES

CHAPTER ONE

1.1 BACKGROUND OF STUDIES

Al-Si-Mg casting alloys are commonly used today because of their properties such as good corrosion resistance, good mechanical properties, good castability, good strength to weight ratio etc. The increased use of cast aluminium alloys in automobile applications such as engine block and cylinder lining materials have created the need for a deeper understanding of service performance and the influence of the processing parameters. In designing cast parts therefore, the alloy designers and process engineers should have an intimate knowledge of how the alloy solidifies at different sections of the cast parts and how it influences the mechanical properties to achieve best service result.

Silicon modifiers Sr and Na were added to change the morphology of the eutectic silicon crystals from large flakes into a fibrous structural morphology. The growth process of eutectic silicon crystal is influenced by these additions and cooling rates variations.

The major purpose of this research work is to investigate the effect of cooling rate and microstructure modification on the mechanical properties of aluminium alloys. Microstructure which is formed during solidification has a significant influence on mechanical properties.

During casting of aluminium alloys, defects are common. These defects usually include micro porosity, shrinkage porosity and cracks.

1.2 PROBLEM STATEMENT

Foundry practice is the starting point for the world's most advanced countries in technological development. All our cast items and designs are products of imagination. The importance of foundry workshop in technical

advancement cannot be over emphasised and hence the study of some of these casting conditions is of paramount importance to this research work. How the thickness of casting in design affects the operating condition of the component produced is very important. Also modified and unmodified morphology of structures produced play a major role in their properties and microstructures and hence must have to be examined.

1.3 RESEARCH OBJECTIVES

The major objective of this research is to examine the effect of different cooling rate and Na/Sr modification on the microstructure and tensile properties of AL-Si-Mg alloy castings. These objectives include

i) To determine how the cooling rates affect the solidification of the alloy

ii) To determine the effect of cooling rate on the grain size of the microstructure

iii) To choose the solidification range that is most appropriate for Al-S-Mg alloys

iv) To relate the cooling rate and modification to the operating conditions of Al-Si-Mg alloys.

These objectives listed above are the driving force for this work.

1.4 SCOPE OF THIS RESEARCH

Referring to the title of this work, this research was limited to the study of properties and microstructures as a result of different cooling rate and modification of alloys during casting. A pattern with different section thicknesses which will replicate to the casting and give it different cooling rates was introduced. The modifications were done by the introduction of sodium,

Na and Strontium, Sr at separate cases. The properties that were studied include:

1 Tensile properties

2 Hardness properties

3 Micro structural analyses

1.5 RESEARCH SIGNIFICANCE

Nigeria is a country in dire need of industrial revolution. Technological and industrial developments of the most advanced countries of the world started from foundry workshop and practice. For Nigeria to follow, we must give priority to research in foundry practices to develop acceptable properties and processes for engineering materials.

CHAPTER TWO

LITERATURE REVIEW

2.1 ALUMINIUM AND ITS ALLOYS (Al-Si-Mg Alloy)

Although rare and expensive a century ago, aluminium has since been identified as the most abundant metal on earth, consisting about 8% of the earth's crust. Aluminium is the third most abundant element known to man after Oxygen and Silicon (sand) which exist in greater quantities.

Sir Humphrey Davy, a British electrochemist established the existence of aluminium in 1808 and about 18years later a Danish scientist, Oersted produced the first tiny pellet of the metal. The next level of discovery of aluminium was the determination of its specific gravity in 1845 by Wohler, a German scientist. He established the lightness of aluminium which is one of the most outstanding characteristics of the metal. He also discovered that aluminium is very easy to shape, was stable in air and could be melted with a blow touch.

Research into aluminium then continued in France where experiments in production techniques enabled Henry Saint-Clair Deville to display a solid bar of metal at the Paris exhibition in 1855. Then aluminium production was very expensive. About 30years later, developments on low cost production of aluminium was geared by two unknown young scientists, Paul Louis Toussaint Heroult of France and Charles Martin Hall of the United States. The two scientists worked independently in their respective countries and in 1886 they almost simultaneously came up with the new process after series of heart-breaking failures and little encouragement.

The first aluminium production companies were founded in 1888, two years after electrolytic process was discovered, one each in France, the United States and Switzerland. In sand castings and majority of industrial processes,

pure aluminium has limited applications. Aluminium and its alloys are widely used in industrial applications. In this research “THE EFFECT OF COOLING RATE AND MODIFICATION ON THE MICROSTRUCTURE AND TENSILE PROPERTIES OF Al-Si-Mg ALLOY”, aluminium-silicon-magnesium alloy was used and not pure aluminium. Commercial cast aluminium-silicon alloys are polyphase materials of composed microstructures belonging to the aluminium matrix. Association classification series 3xxx for aluminium-silicon-magnesium and/or copper alloys and 4xxx aluminium silicon alloys. They are designated by standards such as CEN EN 1706, “aluminium and aluminium alloys”. Castings, chemical composition and mechanical properties are designated in ASTM standards according to the methods of casting.

ASTM B26/B26M “Specification for aluminium alloy sand casting

ASTM B85 “Specification for aluminium-alloy die casting”

ASTM B108 “specification for aluminium-alloy permanent mould casting”

Their use as structural materials is determined by their physical properties (which are primarily influenced by their chemical composition) and their mechanical properties (influenced by chemical composition and microstructures). The characteristic property of aluminium alloy is relatively high tensile strength in relation to density compared with that of other cast alloys, such as ductile cast alloy or cast steel. The high specific tensile strength of aluminium alloy is very strongly influenced by their composed polyphase microstructure.

The silicon content in standardised commercial cast aluminium-silicon alloys is in the range of 5-23wt%. The structure of the alloys can be hypoeutectic, hyper-eutectic or eutectic, which can be determined from the equilibrium phase diagram, Gruzleski and Closset (1990). The properties of a specific alloy can be attributed to the individual physical properties of its main phase

component, that is, 2- aluminium solid solution and silicon crystals and to the volume fraction morphologies of these components.

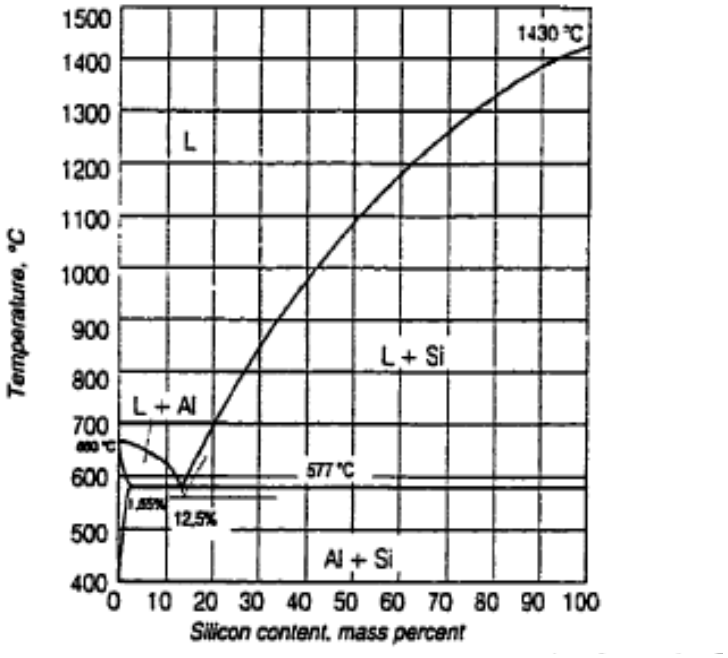

Figure 2.1: Equilibrium binary Al-Si phase diagram. Adapted from Kammer 1999, p86).

2.1.1 HOW AND WHY ALUMINIUM IS ALLOYED

It has been observed that pure aluminium is not used for structural applications. In order to produce aluminium that is of adequate strength for the manufacture of structural components, it is necessary to add other elements to the aluminium. It will be very unusual to find pure aluminium (1xxx series) chosen for structural fabrication because of their strength characteristics. Although 1xxx series are almost pure aluminium, they will respond to strain hardening especially if they contain appreciable quantity of impurities such as silicon and iron. However, even in the strain hardened condition, 1xxx series alloys have very low strength when compared to other series of aluminium alloys such as 3xxx and 4xxx. Most times 1xxx series are

chosen for their superior corrosion resistance and/or their high electrical conductivity. The most common applications for 1xxx series alloys are aluminium foil, electrical bars, metalizing wire, chemical tanks and piping systems.

The addition of alloying elements to aluminium is the principle methods to produce a selection of different materials that can be used in a wide variety of structural applications. The major aluminium alloy series are:

Series	principal alloying element
1xxx	aluminium 99% greater
2xxx	copper
3xxx	manganese
4xxx	silicon
5xxx	magnesium
6xxx	magnesium and silicon
7xxx	zinc

2.1.2 THE PRINCIPAL EFFECTS OF ALLOYING ELEMENTS

Only the effect of silicon and magnesium on aluminium matrix was considered because this project is carried out with Al-Si-Mg alloy.

Silicon (Si) 4xxx: The addition of silicon particles to aluminium matrix reduces the melting temperatures of aluminium and improves its fluidity. Silicon along in aluminium produces a non heat treatable alloy; however, in combination with magnesium it produces a precipitation hardening heat treatable alloy. Consequently, there are both heat treatable and non heat treatable alloys within the 4xxx series. Silicon additions to aluminium are commonly used for the production castings. The most common applications for the 4xxx series alloys are filler wires for fusion wielding and brazing of aluminium.

Magnesium (Mg) 5xxx: the addition of magnesium to aluminium increases strength by solid solution strengthening and improves their strain harden-ability. These alloys are the highest strength non heat traceable aluminium alloys and are therefore used extensively for structural applications. 5xxx series alloys are produced mainly as sheet metal and plate and occasionally as extrusions. This is in order that these alloys are train hardened quickly and therefore difficult and expensive to extrude. Some of the common applications of 5xxx series alloys are truck and train bodies, buildings, armoured vehicles, ship and boat buildings, chemical tanks, pressure vessels and cryogenic tanks.

Magnesium and Silicon 6xxx: The addition of magnesium and silicon to aluminium produces the compound magnesium silicide. The formation of this compound provides the 6xxx their heat treatability. The 6xxx series alloys are easily and economically extruded and for this reason are most often found in an extensive selection of extruded shapes. These alloys form an important complementary system with the 5xxx series alloys. The 5xxx series alloy used in the form of plate and 6xxx are often joined to the plate in some extruded forms. Some of the common applications for the 6xxx alloys are hand rails, drive shafts, automotive frame sections, bicycle frames, scaffolding, stiffeners, and many other structural applications.

2.1.3 PROPERTIES OF ALPHA-ALUMINIUM SOLID SOLUTION

The alpha aluminium solid solution is the matrix of cast aluminium-silicon-magnesium alloy. It crystallizes in the form of non faceted dendrites, on the basis of crystallographic lattice of aluminium. It is a face centred cubic (fcc) lattice system and noted by the symbol A1, with co-ordinate number of 12 and with four atoms in one elementary cell. Lattice A1 is one of the closest packed structures, with a very high filling factor of 0.74. The plane of the closest filling

is the (111) plane and (110) direction is the closest filling direction in this lattice. The atoms are bounded by metallic bond characterised by isotropy and relatively low bonding energy.

2.1.4 PROPERTIES OF SILICON CRYSTAL

The silicon precipitates, present in commercial aluminium silicon alloys, are almost pure, faceted crystals of this element. The silicon crystals can have different morphologies such as primary, compact, massive precipitates in hypoeutectic alloys or branched plates in aluminium-silicon eutectic.

Silicon crystal lattice is symbolised by A4, cubic structure of diamond type. Each atom is bounded by four other atoms with covalent bond, thereby forming a tetrahedron. Eight tetrahedron form one elementary cell of A4 lattice, face centred with four additional atoms from the centre of each tetrahedron. This structure is less closes packed than A1 lattice and hence has smaller filling factor of about 0.34.

2.2 ALLOY MODIFICATIONS

The addition of titanium in various forms into aluminium alloys has been found to serve a strong effect in nucleating the primary aluminium phase (Flood and Hunt 1981). It is instructive to consider the way in which this usually happens. Titanium in solution in the liquid metal at a concentration above about 0.15 weight percent would be expected to be precipitated as $TiAl_3$ in the peritectic reaction. There is no doubt that $TiAl_3$ is an active nucleus for aluminium because $TiAl_3$ is found at the centre of aluminium grains, and there is a well established orientation relationship between the lattices of the two phases. In this system, Ti can be regarded as a grain refiner and hence a nucleating agent, even at concentration below 0.01% Ti.

2.2.1 MODIFICATION OF THE Al- Si EUTECTIC BY Na AND Sr

When Al-Si alloy systems are modified, the eutectic silicon is seen on polished sections to consist of coarse plates with sharp edges. These usually have been thought to be detrimental to mechanical properties because they are thought to act as crack initiation sites. Because of this, for alloys containing above about 5-7% of Si, the addition of sodium (Na) or strotium Sr to the melt has been favoured to refine the eutectic Silicon phase.

The action of modification was first explained by Flood and Hunt, (1981). They interrupted the solidification of unmodified and sodium modified Al-Si eutectic alloy to study the form of the growth front in a slice of a cylindrical casting. Also the growth morphology of strontium Sr modified structure was investigated, Hawell (1987).

In the case of the unmodified alloy, the growth form appeared dendritic, with some nucleation apparently ahead of the freezing front. But in the case of sodium modified alloy, planar growth of the eutectic front was stabilised with an effective length of solidification front, a factor of 17 times shorter than the dendritic front. Thus for some given quantity of heat extracted by the mould over a given area, the interface in the case of the planar front would advance at 17 times the rate, and therefore have a much finer structure than the unmodified alloy.

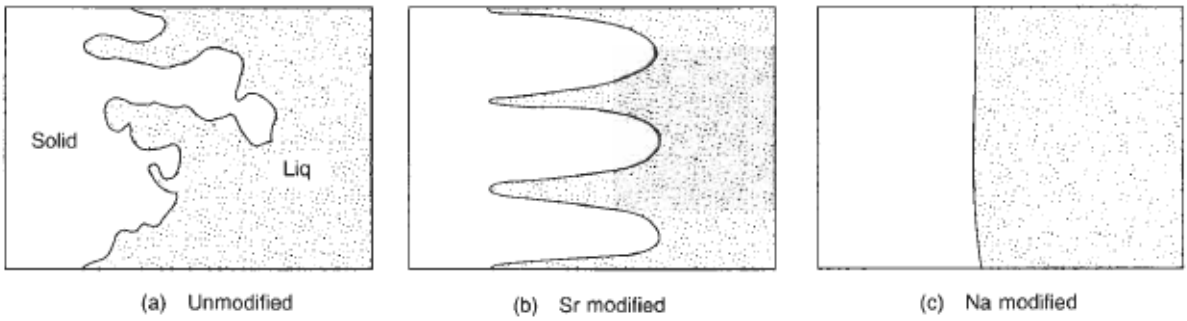

Figure 2.2: Growth morphology of a) Unmodified alloy b) Sr modified c) Na modified (Extracted from Flood and Hunt 1981)

Interestingly, the form of freezing front for the Sr- modified eutectic alloy is cellular, the freezing condition commonly found in sand castings. The intermediate condition explains the intermediate performance of Sr. The cellular pattern, resembling a honey comb is seen occasionally on the surface of Sr modified castings that have suffered some degree of poor feeding, encouraging the loss of some residual liquid from around the cell and so giving slight depressions on a cast surface that outlines the cell boundaries. The cellular structure of the front does lead on other occasions to some problem to feed Sr modified alloy casting, as contrasted with those cast from Na modified alloy. Surface initiated porosity is also favoured by modifications with Sr where as it is discouraged by modifications with Na. The choice between the use of sodium or strontium depends on the circumstances. Sodium is usually lost from a melt within a time of the order of 15 to 30 minutes as a result of evaporation. Strontium, on the other hand, is a normal, stable alloy in liquid Al alloys. Although it is slowly lost by oxidation at the surface, and sometimes can soak away into refractory furnace linings until they saturate, the alloy will usually survive several remelting.

The addition of the strontium is an expensive option, but it is taken in an effort to improve ductility of the casting alloy. However, the results are not always straight forward to understand. Much confusion has existed over whether strontium can be successfully added without the deleterious effect of hydrogen pick-up. Gruzleski has carried out careful laboratory measurement on Al-7Si-0.36Mg alloy and found no increase in the rate of absorption of hydrogen after additions of strontium. Thus, when undisturbed, the melt may continue to be protected from the environment by its oxide.

Small amounts of Sr can transform the morphology of the eutectic silicon phase present in Al-Si casting alloys from coarse plate-like to fine fibres

networks. The strontium distribution was studied in atomic resolution by probe tomography and in nanometre resolution by transmission electron microscopy. The combined investigations reveal that Sr co-segregates with Al and Si within the eutectic Si phase. Two types of segregations were found, viz.

Nanometre- thin rod-like co-segregations type1 are responsible for the formation of multiple twins in a Si crystal and enable its growth in different crystallographic directions.

Type two segregations come as more extended structures, restrict growth of a silicon crystal and control its branching.

2.3 SILICON MORPHOLOGY

Porous materials are generally obtained by localized electrochemical corrosion under anodic polarization. Lu and Hellawell (1987) have demonstrated the evolution of silicon morphology. Impurities can have a very strong effect on the morphology of grain boundaries. For instance, it is well established that segregation at grain boundaries in the wide range of materials promotes the formation of new grain boundary configuration such as faceting. Perhaps very little is known about the crystallographic structure of chemically modified boundaries.

Determination of the atomic structure of pure symmetrical-tilt high-angle coincident boundaries in silicon and germanium by high resolution election microscopy has firmly established that such boundaries assume symmetrical morphology in their equilibrium configuration. The porous silicon exhibits strong photoluminescence in the visible range instead of the weak luminescence of bulk silicon. The porous silicon exhibits distinctive appearance. The size of the structure varies by three orders of magnitude, ranging from nonporous silicon (including microporous and mesoporous

silicon) with pores and crystallites in the nanometre scale, up to macro porous silicon with pore and pillar dimensions in the microscale. Generally, porous silicon formed P-Si and n-Si have distinctive differences in terms of pore size, orientation and degree of branching. Because of the intricate relations among the kinetic factors and geometric elements, the detailed features of porous silicon morphology and the mechanisms for their formations are complex and greatly vary with each situation.

Aluminium alloys with silicon as a major alloying element consist of a class of alloys, which provide the most significant part of all shaped castings manufactured, especially in automotive industries. Silicon has an outstanding effect in the improvement of casting characteristics, combined with other physical properties such as mechanical properties and corrosion resistance and hence study of its morphology is very crucial. Various silicon morphologies can also affect t he function of the silicon in the alloy system. Since the strength and hardness of alloys depend mainly on their microstructure. The mechanical properties of Al-Si alloys depend to a great extent on the size and morphology of eutectic silicon particles.

Under normal conditions, the silicon particles are present as coarse acicular needles Okorafor (1986). These needles act as crack initiation and weaken the mechanical properties significantly. The quality of the microstructure of aluminium parts depends on the chemical composition, melting process, casting process and solidification rate.

The morphology of the silicon phase is either plate-like or fibrous, depending on whether the melt has been treated with modifiers such as sodium or strontium. On a two dimensional metallographic view, the silicon

rod-like particles and the silicon plate look like rods. Therefore, to describe the morphology of silicon phase, we need parameters such as silicon rod diameter, spacing and length.

The effects of silicon on aluminium alloys are well known; increased fluidity, decreasing casting shrinkage and improved wave resistance. Silicon has fan shaped morphology in metallographic section. This type of eutectic structure also known as lamellar structure, impacts poor mechanical properties compared with the modified structure of the casting.

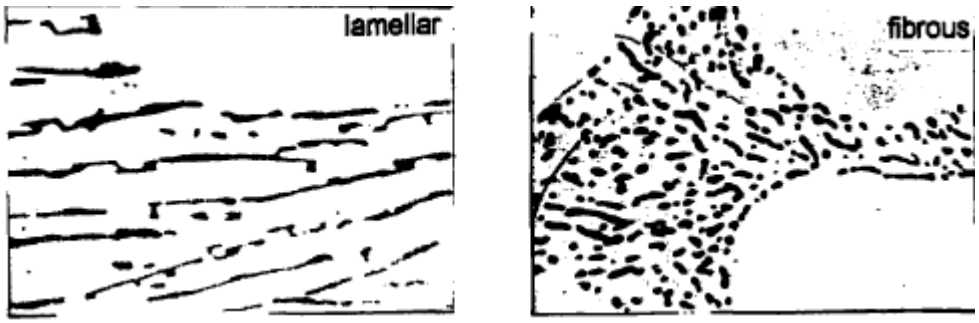

Figure 2.3: Lamellar and fibrous structures of silicon in Al-Si alloys X800 (Extracted from Gruzleski and Closset, 1990, p40, 41).

Small additions, maybe up to 0.02% Emadi, Toguri and Gruzleski (1993) of elements such as sodium, strontium, antimony and cerium called modifiers, completely change the morphology of the silicon eutectic phase from large flakes to a fibrous structure. Several attempts have been made to explain the mechanism of modification in the past. Hellawell explained formation of fibrous silicon by assuming that atoms of the modifying elements adsorb on and disturb the growth step of the silicon crystal. These activities cause repeated twining and hence the fibrous structure of the silicon phase. These modifying elements have very strong affinity for silicon and have form chemical compounds that remain on the surface of the silicon crystal, perturbing the normal growth form and act as nucleation sites to produce a

fibrous structure. Addition of these elements is very important but the quantity added should be limited to 0.02%.

2.4 CASTING PROCESSES

Metal casting is majorly classified based on the mould system that is involved. Based on this, they are categorised into the following:

2.4.1 EXPANDABLE MOULD CASTING

Expandable mould casting is a type of casting process where the mould is destroyed when the casting solidities. They are single use mould process where a new mould must be prepared for each casting. Example of expandable mould casting process includes: green sand casting, co_2 sand casting, shell sand casting, investment casting, full mould casting, etc. This project is carried out with green sand casting using clays as binders and different moulds are designed to give different cooling rates

2.4.2 NON EXPANDABLE MOULD CASTING

These are types of casting process where the mould is not destroyed after solidification of the casting. The moulds are made from metallic materials. They are also called permanent mould casting. Here the casting is made by pouring molten metal into a mould made of some metallic alloy or any other material of permanence. Permanent moulds are costly and are recommended for mass production of castings. One of the problems associated with non expandable or permanent mould casting is that they are impractical for large casting and alloys of high melting temperatures, but can be advantageous for small and medium sized non ferrous castings.

The iron and steel mould are suitable for non ferrous casting, while steel moulds coated with refractory materials such as graphite, are successfully used for the production of iron casting. The casting produced by these moulds require less skills, have improved surface finish, high dimensional occupancy and less number of rejection by sand casting.

We also have semi permanent mould casting where sand cores are used at some point, instead of metallic cores. The use of sand cores result in lower cost and also allow core openings of irregular shapes and undercuts of such type where metal cores will be too expensive and difficult to handle on production basis.

We have special casting processes which may include:

2.4.3 INVESTMENT CASTING

This is also called lost wax process or precision casting. The term investment refers to the cloak or special covering apparel in some cases a refractory mould, surrounding a refractory covered wax pattern. In this process, a wax pattern must be made for every casting and gate system for example, the pattern is expandable. Investment casting produces very high surface quality and dimensional occurancy. The casting produced by this method are within very close tolerances and do not require subsequent machining. Investment casting has step by step procedures which must be followed to produce sound castings. Investment casting produces extremely smooth surfaces with very close tolerances that can easily be maintained in average work. It eliminates most machining operations and is adoptable in all metallic alloys. Shapes with undercuts, intricate shapes and mass production are suitable with this casting process. Conversely, large objects are impracticable with this process.

2.4.4 CONTINUOUS CASTING

Continuous casting is generally employed for the production of bars, rods, squares, pipes, tubes, sheets, etc. It consists of pouring the molten metal into the upper end of a long vertical metal mould (open at both ends) and cooling rapidly by water. The solidified casting is withdrawn by gravity in a continuous length from the lower end of the mould. Continuous casting utilizes two major processes Asarco process in which the molten metal is fed through gravity pull, into the mould line with graphite, and reciprocating process in which the copper mould reciprocates up and down with the surrounding water jacket. In the second process, the molten metal is poured into the mould at uniform speed through a pipe connected to the furnace.

2.4.5 SHELL MOULD CASTING

The shell moulding process also called croning process consists of making a mould that has two or more thin shell like ports consisting of thermosetting resin bounded sand. The resins may include phenol-formaldelydes, urea formaldelydes and poly esters. It is mixed as a sand as powder from 3 to 10% by weight. It may be applied as a liquid then dried on the sand grains. The mixture for moulding must be dry and free flowing. A very smooth surface is generally obtained and dimensional accuracy of this process reduces cleaning and machining costs. But resin binders are more expensive than other binders. Also initial cost of metal pattern is high in this process.

2.4.6 DIE CASTING

The die casting also known as the pressure die casting may be defined as the casting which uses the permanent mould called die and the molten metal is introduced into it by means of pressure. The casting produced by die casting

process is good and requires very little machining. The dies are usually made in two parts which must be locked severally before molten metal is forced or pressed into them under high pressures of between 7mpa and 700mpa. The pressure may be achieved by the application of compressed air or by hydraulically operated pistons. Ferrous alloys are not commercially die-cast because of their high pouring temperatures. Two major types of die casting are hot chamber die casting and cold chamber die casting. In hot chamber die casting machine, the molten metal is forced in the die cavity at pressures from 7 to 14 mpa which may be obtained from the application of the compressed air. In the cold chamber die casting machine, the melting unit is usually separate and molten metal is transferred to injection mechanism by ladle, here the pressure may range from 20 to 210 mpa and sometimes up to 700 mpa. The greater pressure in cold chamber die casting machine is applied to compensate for reduced fluidity resulting from low pouring temperature. Rapid and economic production of large quantities of identical parts can be achieved. Little machining is required and parts having thin and complex shapes can be cast accurately with ease. In this process the cost of equipment is high and special skill is required.

2.4.7 CENTRIFUGAL CASTING

This is another type of casting used in industries. Centrifugal casting is used in automobile companies in the production of cylinder lining materials, pistons and rings of internal combustion engines. It is a casting process in which molten metal is poured and allowed to solidify while the mould is revolving. The castings produced under this centrifugal casting are called centrifugal casting. Centrifugal casting is divided into the following:

1 True centrifugal casting which is especially employed for casting articles of symmetrical shapes. Example cast iron pipes, sleeves, steel gun barrels, etc.

2 Semi-centrifugal castings which is majorly applied for making large sized castings which are symmetrical about their own axis such as pulleys, disc wheels, gears, propellers, etc.

3 Centrifuging casting - casting of irregular shapes which can produce by a large number of small sizes casting at one time.

2.5 SOLIDIFICATION PROCESSES

In solidification, how the metal changes states from liquid to solid and how the solid farther develops its structure by solid state transformations, together with its pore structure due to the precipitation of gas was considered. In this section, some of the solidification processes that are involved in sand casting were looked into.

2.5.1 NUCLEATION

The solidification of metals occurs by nucleation and subsequent processes. The same also applies to melting which is opposite of solidification but with one important difference which is that nucleation of solid phase during freezing is much more difficult process than the formation of nuclei of the liquid phase during melting process. The solidification is important because it controls the structure and hence the properties of casting. As the liquid metal cools below its freezing temperature, the thermal agitations of the particles decrease. As the under cooling process progresses, small group of atoms move to a crystalline arrangement and form clusters of atoms in some locations in the melt. These clusters form nuclei on further cooling. Initially as

the temperature of the liquid metal is reduced below its freezing point, nothing happens and this is due to the nucleation problem associated with conversion of clean liquids to the solid phase. But as the temperature drops further, the thermal agitations of atoms reduces and allowing small random movement of atoms to form clusters. It is important to note that it is not all the clusters that form will grow to form various nuclei for the solidified metal. In order words, some of these clusters will dissolve and go back to the liquid by thermal agitation. It is only those clusters with maximum critical energy that will nucleate and grow as the temperature of the melt decreases further. For small nuclei, the resultant energy to form new phase during growth is expressed as its volume (v) energy and free energy per unit volume (ΔG_v). This is also proportional to the surface area and solid/liquid surface energy (Υ). Assuming that the nuclei formed from the clusters are spherically shaped, the free energy for nucleation is given as, Poter and Esterling (1981),

$$\Delta G = 4\pi r^2 \Upsilon - \frac{4r^3 Gv}{3} \quad \text{.....1}$$

Where ΔG_V = Volume free energy

Υ = The solid/liquid interfacial free energy

R = Radius of the nuclei

It is again worth noting that there is a minimum radius which the nuclei must reach before growth will take place. This minimum radius is also called critical radius of the nuclei. The critical radius is obtained by differentiating the expression for free energy, that is, differentiating equation (1) with respect to radius, r

$$\frac{d\ (\Delta G)}{dr} = \frac{d(4\pi r^2 \Upsilon)}{dr} - \frac{d(4r^3 \Delta Gv)}{dr}$$

But $\frac{d(\Delta G)}{dr} = 0$

Then $8\pi r\gamma - 4\pi r^2 \Delta G$

So that $2\gamma = r\Delta G_v$

or $r^* = \frac{2\gamma}{\Delta G}$.....(2)

All the nuclei that do not reach this critical radius and maximum energy will dissolve back into the liquid metal. As the temperature of the melt drops further, nuclei above critical radius will grow and this is accompanied by decrease in energy of the system.

Basically, there are two major types of nucleation, homogeneous nucleation and heterogeneous nucleation. In homogeneous nucleation, atoms of the metal itself provide sites for nucleation. But when the crystallization begins to form on impurities, particles, nucleation agents and on the mould walls, it is called heterogeneous nucleation. Heterogeneous nucleation is what is obtainable in industrial practices of foundry. Heterogeneous nucleation is common in alloy casting processes, in which foreign particles and the mould walls are the major nucleation sites. In commercial foundry practices, nucleation agents called inoculants are added to many molten alloys to increase nucleation sites thereby producing a fine grained structure. Some of these inoculants are titanium and boron for aluminium alloy casting.

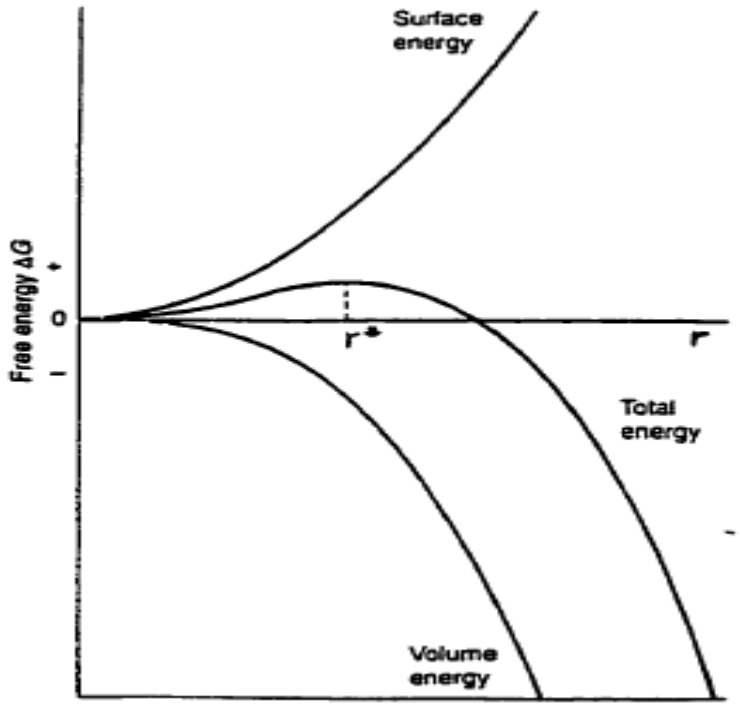

Figure 2.4: Variation of free energy ΔG with radius of nucleus r. r* is the critical radius of those nuclei which will grow (Extracted from Porter and Eesterling, 1981, p266).

We can also calculate the number of grains nucleated within a given melt volume and time. This is called nucleation rate or rate of nucleus formation. If N_n is the number of crystalline clusters, which each contains n atoms and N_l is the number of atoms in the liquid (when Nn << Nl), nucleation rate can be written as

$$N_n/N_l = \text{Exp-}(\frac{\Delta Gn}{K\beta T}) \quad \text{.....3}$$

It has been observed that cluster formation and distribution depend largely upon temperature.

2.5.2 GROWTH

Nucleation and subsequently growth processes of solidification involve extraction of heat from the melt in more or less controlled manner. It has been

shown that the movement of the boundary separating a liquid from solid crystalline phase, under a temperature gradient normal to the boundary, may be considered the resultant of two different atomic movements. At the interface, those atoms that leave the liquid and join the solid determine the rate of attachment while those that move in opposite direction determine the rate of detachment.

When the molten metal is poured into a cold mould, the metal at the mould surface cools more rapidly and heterogeneous nucleation starts on the mould wall. Due to the rapid cooling because of large temperature gradient between the liquid metal and mould wall, the region close to the mould wall will have fine grains which have equiaxed morphology called the outer equiaxed zone Kurz and Fisher (1989).

After nucleation, solidification process will only proceed if heat is extracted through the solid, cooling the advancing melt front below the equilibrium freezing temperature. The growth rate is dependent on the rate of heat extraction. In other words, as the rate of heat extraction increases, the temperature of the solidification front falls and the growth rate (G) increases. The driving force for growth during solidification is undercooling. For a pure metal, the growth morphology at the solidification front is planar. But at high growth rate, cellular solidification morphology can also develop. At a very high cooling rate, the cell grows rapidly and the advancing projections have complex tree-like geometry called dendritic solidification.

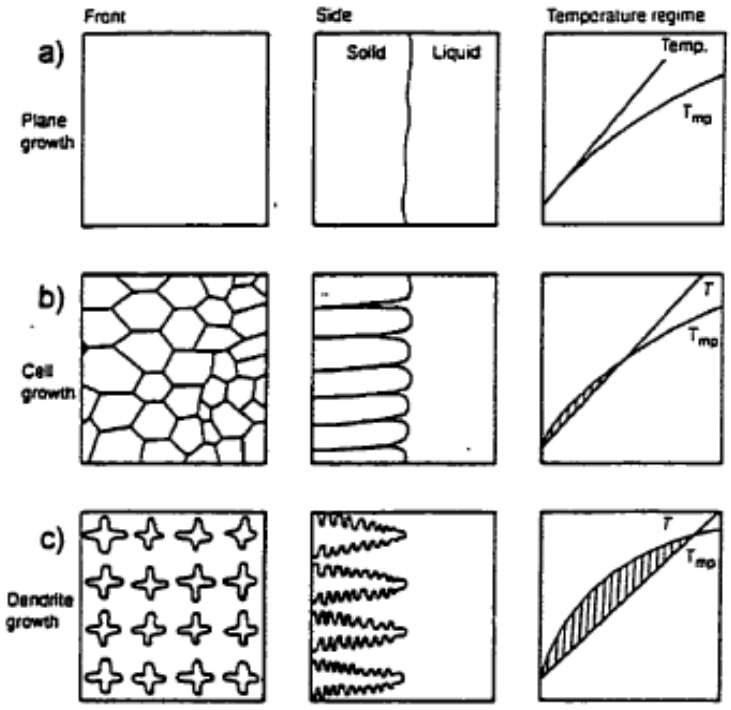

Figure 2.5: Transition of growth morphology from (a planer (b cellular (c dendritic as compositionally undercooling increases. (Extracted from Campbell, 1991, p143).

A heat balance equation for the solidification process can be written as

$K_sG_s = K_lG_l = \rho_S\Delta HR$..... (4)

Where Ks = thermal conductivity of the solid in J/cmdeg.s

K_l = thermal conductivity of liquid in J/cmdeg.s

Gs = temperature gradient in the solid at the solid liquid interface in deg/cm

G_l = temperature gradient in the solid at the solid/liquid interface in deg/cm

R = Growth rate

ΔH = heat of fusion in j/g.

Maximum growth rate occurs when temperature gradient in the liquid at the solid/liquid interface approaches zero, that is,

$G_l \rightarrow 0$ maximum growth occurs and hence

$R_{max} = K_s G_s / \rho_s \Delta H$.....(5)

Where R_{max} = maximum growth rate.

However, the best crystals are usually produced when the growth rate is low. The ratio of nucleation rate (N) to the growth rate (R) determines the grain size. When the N/R ratio is high, a fine grain size is produced but if the ratio is low, a coarse grain size will result.

2.5.3 DENDRITIC SOLIDIFICATION

Dendritic solidification is the most common form of solidification in casting. The growth rate into the liquids depends on the crystal orientation, and it is only those that have a rapid growth direction normal to the mould wall will survive the growth process and these grains are columnar in shape (columnar dendrites). In the metallurgy of wrought aluminium, it is the grain size of the alloy that is usually the important structural features. Secondary dendrite arm spacing (DAS) is the most important structural length parameter. The mechanical properties of most cast alloys are seen to be greatly dependent on the secondary arm spacing, DAS.

In general practice, the columnar grains grows from the surface of the interior, with equiaxed grains (equiaxed dendrites) at the centre of the melt. In this process, small pieces of the dendrite arms are separated from the dendrite and swept into the centre and this occurs when the heat released at the solid/liquid interface is sufficient enough to raise the temperature locally, thereby causing the side arms to melt. Now these small crystals move into the centre of the casting to serve as the nuclei for the formation of the equiaxed grains. During the growth process, dendrite arms will unite together forming a single crystal lattice called grain. The grain may contain thousands of dendrites.

A decrease in dendrite arm spacing (DAS) is accompanied by an increase in ultimate tensile strength and ductility.

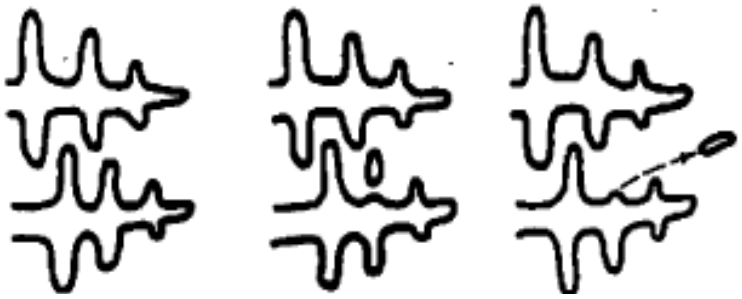

Figure 2.6. Schematic of the side arm remelting of a dendrite and movement to the center to serve as a nucleus for an equiaxed grain. (Extracted from Brooks, 1982, p82).

It is further revealed that the dendrite arm spacing (DAS) is directly proportional to the local solidification time t_f, which is the interval between liquidus and solidus temperatures in the cooling curve, Gruzleski (2000). Secondary dendrite arm spacing is the average spacing between the secondary dendrite arms and is determined by the linear intercept method.

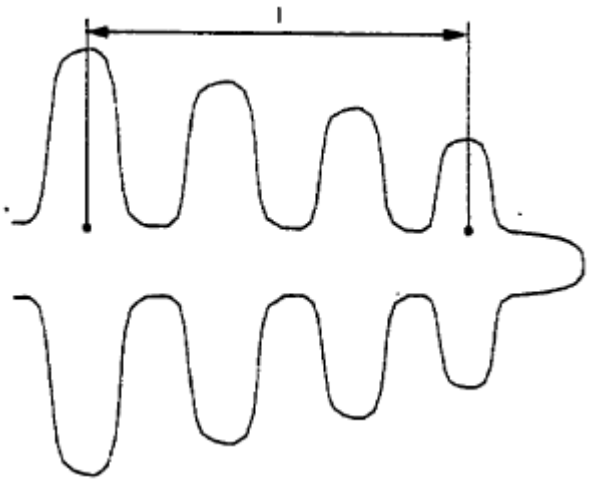

Figure 2.7: Measurement of dendrite arm spacing, DAS (Extracted from Gruzleski, 2000, P113).

Dendritic solidification is a diffusion controlled phenomena and for many alloys, an empirical relationship exists between dendrite arm spacing and local solidification time, t_f

That is, DAS $=at_f^{n1}$ .....(6)

Where a = constant for an alloy

t_f = local solidification time

n1 = constant with value between 0.3 and 0.5

Considering the mechanism for coarsening of dendrites, dendrite arms form at the very small spacing near the top of the main body or the primary arm. With some time, the dendrites try to reduce their surface energy by decreasing their surface area. And this causes the small arms to go back into the solution and the large arms to grow. The rate of dendrite coarsening tends to be limited by the rate of the solute in the liquid, as the solute transfers from the dissolving arms to the growing arms. As the cooling rate is decreased and dendrite arm spacing grows, the ultimate strength decreases until it reaches the yield strength. This causes fracture of the alloy due to brittleness.

2.5.4 COOLING CURVE

The cooling curve is the temperature time dependent relation obtained during the modification of metal or an alloy in the mould Gruzleski (1995). Cooling curve is a powerful tool used to study transformations occurring during the solidification process. The ideal cooling curve for a hypoeutectic or hypereutectic alloy is shown in the figure below

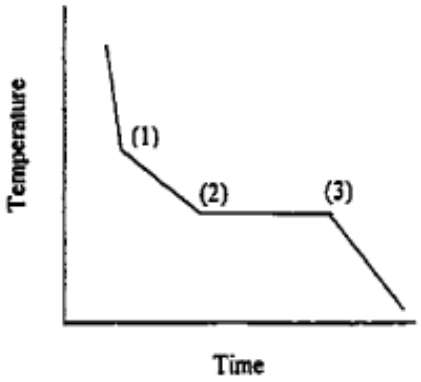

Figure 2.8: An ideal example of a simple cooling curve for a hypo or hyper eutectic alloy, (extracted from Gruzleski, 1995).

In the figure above, solidification of the primary phase starts at point 1 while the eutectic solidification starts at point 2. After the release of the latent heat at this point, the cooling continues at a constant temperature. Finally, the solidification is completed at point 3. Below point 3 is where we have solid state transformations. But in real foundry practice, the cooling curve does not represent the ideal situation depicted by the curve above. In real situation, the solidification rate is extremely high and reactions do not begin exactly at the equilibrium freezing temperature. Therefore, it is necessary that the temperature drops below the equilibrium value to give enough time for the nucleation process. This phenomenon is called undercooling.

2.5.5 COOLING RATE

Cooling rate of a solidifying alloy can be defined as the rate of removal of heat (extraction) from the liquid metal as it solidifies. The cooling rate shows the rate of change of temperature over time during solidification. The cooling rate may be obtained at any temperature from the temperature-time cooling curve by drawing a tangent to the curve at the temperature and determining the value of slope for the tangent, Avner (1974).

2.6 SOLIDIFICATION HEAT TRANSFER

In casting, heat extraction changes the energy of the phases, Kurz and Fisher (1989), (solid and liquid) in two ways:

1. There will be decrease in enthalpy of the liquid or the solid, due to cooling given by $\Delta H = \int CdT$.....(7)
2. There will also be decrease in the enthalpy of the system due to the phase transformations from liquid to solid. This is equivalent to the latent heat of fusion; ΔH_f. Removal of heat is achieved by applying suitable means of cooling to the melt in order to create an external heat flux q^-_e. The heat fluxes will determine the direction of heat flow between the system and the surrounding. The hot liquid metal takes time to loose its heat and solidify. The rate at which the liquid metal can lose heat is the cooling rate, dT/dt that is, change in temperature per unit time. This cooling rate is controlled by a number of resistances to heat flow, Flemings (1974).

   Some of the resistances to heat flow from the system through the casting to the surrounding are

   a) The liquid
   b) The solidified metal
   c) The metal/mould interface
   d) The mould
   e) The surrounding of the mould

   There are different types of solidification heat transfers in sand casting technique. They include

   a) Heat transfer by conduction
   b) Heat transfer by convention
   c) Heat transfer by radiation

2.6.1 CONDUCTION HEAT TRANSFER

Conduction is the most common and dominant mode of heat transfer during solidification, Poirier (1994). Conduction is the mechanism in which that heat is transferred internally with the solidifying metal and the mould. The most predominant is the steady state temperature distribution between the metal and the mould wall. It can be represented schematically as the steady state temperature distribution in a plane wall and the heat conducted from left to right in the figure below.

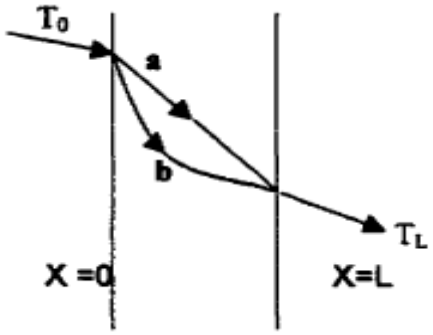

Figure 2.9: Temperature distribution in a plane wall, (a) Linear transient (b) Non- linear transient

At x = 0 the surface is hotter than the surface at x = L. Therefore, heat moves from surface at x = 0 to the surface at x = L thereby giving rise to heat flow and temperature gradient. Therefore, one can say that $Q = K_A/L\ (T_O-T_L)$.....(8)

Where Q = heat flow rate in W

A = area of the plate in cm^2

L = thickness of the plate in cm

T_o, T_L = temperature in ^oC

K = thermal conductivity of the plate in W $cm^{-10}c^{-1}$

Equation (8) can be rewritten as a function of heat flux. Thus

$Q = -k\frac{dT}{dx}$ ..... (9)

Where q = heat flux in W cm^2

$\frac{dT}{dx}$= temperature gradient in ^{0}C/cm

The temperature distribution is linear only when a steady state predominates as shown by line 'a' in the figure above. But when the situation is transient, the temperature distribution is non linear as indicated by line 'b' in the figure above.

For the transient of non linear distribution

$$\frac{\partial q}{\partial x} = -\rho C_p \frac{\partial T}{\partial x} \quad \text{..... (10)}$$

Where ρ = density in g/cm^3

C_P = heat capacity in J/g/^{0}C

2.6.2 ENERGY EQUATION FOR CONDUCTION

When we combine equations 9 and 10, we obtain energy equation for conduction heat transfer. Thus we have

$$\frac{\partial T}{\partial x} = \alpha \frac{\partial^2 T}{\partial x^2} \quad \text{..... (11)}$$

Where α is called thermal diffusivity (cm^2/s) and is defined as $\alpha = k/\rho C_p$ .....(12)

2.6.3 CONVECTIVE HEAT TRANSFER

Convection is the bulk movement of the liquid metal during casting under the driving force of the density differences in the liquid, Cole (1971). It is a mass transport phenomenon where particles are carried by fluid over some distances.

The existence of convection has been cited as important because it affects the columnar to equaixed transition, Kurz and Fisher (1989). In most castings, grain structure is much less important than soundness and it seems to be little known that convection can give severe soundness problems. The

problem of convection flow in casting can create serious problem in counter gravity filling systems. Convection driven by solutes can raise a number of problems viz heavy solutes cause the liquid to sink, and higher solutes cause floatation Geiger and Poirier (1973). Complex problems involved in convective heat transfer during solidification are outside the scope of this research probably due to lack of equipments and texts.

2.6.4 SOLIDIFICATION OF CASTING IN SEMI-INFINITE SAND MOULDS

When a pure liquid metal at its melting point, T_m is poured into the sand mould, a temperature gradient develops in the mould wall and transfer of heat from the metal of the mould wall causes rapid freezing of the metal close to the mould wall and have evolution of latent heat of solidification. Evolution of latent heat determines the rate of advancement of the solid/liquid interface into the liquid metal. So if the mould design can be considered to be semi-infinite in thickness, the thickness of the solidified metal layer (m) at time (t) can be related as follows, Gaskel (1992)

$$M = \frac{2}{\sqrt{\pi}} \frac{Tm - To}{\rho s H} (k_m \rho_m C_m)^2 t^{1/2} \quad \text{.....(13)}$$

Where M = thickness of solid metal in cm

T_m = melting temperature of the metal in ^0C

T_o = sand moulding temperature in ^0C

ρ_s = density of solid metal in g/cm^3

H = latent heat of the metal in j/g

K_m = thermal conductivity of the mould in $W/cm/^0C$

ρ_m = bulk density of the mould in g/cm^3

H_m = heat capacity of the mould in $j/g/^0C$

t = total solidification time

This relationship was developed by Gaskell and can be represented by the figure below.

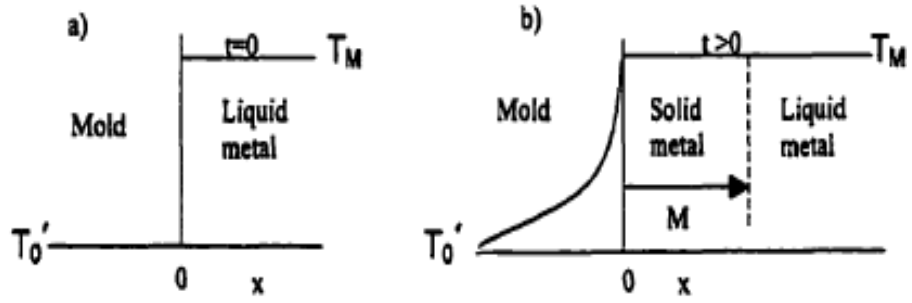

Figure 2.10: Temperature profile during solidification of liquid metal constrained in a sand mould; (a) at t = 0 and (b) at t > 0 (Extracted from Gaskell, 1992, p402).

From equation 13 above, Flemings (1974) the term $K_m\rho_m c_m$ is called the heat diffusivity of the mould and measures the ability of the mould to absorb heat. As a result, the amount of solidified metal depends on the properties of the metals and the heat diffusivity of the mould.

2.6.5 COEFFICIENT OF HEAT TRANSFER

When the liquid first enters the mould, the macroscopic contact between the metal and the mould wall is good because of the conformance of the molten metal. But at microscopic view, gaps exist between the high spots where there are asperities. At these high spots, the high initial heat flux causes nucleation of the metal by localised severe under cooling and the solid then spreads to cover most of the surface of the casting. Poirier (1994), modified equation 13 by considering the general heat transfer coefficient (hg), which accounts for the heat resistance that exists in the gap between the metal and the mould. A modifying factor (ϕ) to account for resistance to heat transfer due to metal/mould gap in sound moulds was developed.

$$\emptyset = 1 - \frac{\sqrt{\text{Km}\rho\text{mcm}}}{hg}\sqrt{\pi}\,\text{t ln } 1 + \frac{hg\sqrt{\pi t}}{\sqrt{\text{Km}\rho\text{mcm}}} \quad \text{.....14}$$

Where hg = heat transfer coefficient in w/cm^{30}cV

T = total solidification time in sec.

Thus, equation 13 can be written as

$$M = \frac{2\pi}{\sqrt{\pi}} \frac{\text{Tm} - \text{To}}{\rho\text{sH}} (\text{Km}\rho\text{mcm})^{1/2} t^{1/2} \quad \text{.....(15)}$$

2.6.6 CHVORNIOV'S RULE

Chvorniov developed an expression for total solidification time considering the dimensions of the mould, Chvorniov (1940). If the volume of the casting is v and the surface area of the mould is A, thickness of the mould m can be replaced by v/A, which is the modulus of the castings. He discovered the total solidification time of the casting t to be

$$t = \frac{\pi}{4\emptyset^2}\left(\frac{\rho s}{\text{Tm}-\text{To}}\right)\left(\frac{1}{\text{Km}\rho\text{mcm}}\right)\left(\frac{V}{A}\right)^2 \quad \text{.....(16)}$$

$$\text{or } t = C\left(\frac{V}{A}\right)^n \quad \text{.....(17)}$$

This is chvorniovs's rule where c is chvornior's constant and n is also constant ranges between 1 and 2. Under an ideal condition of solidification, n=2, it assumes

a) Isotropy and homogeneity of semi-infinite casting

b) Absence of super heat

c) Pure or eutectic alloy and

d) Constant metal/mould interface temperature.

But in real and practical condition, n assumes a value between 1 and 2, Tiryakioglu, Askeland and Butler (1998).

Okorafor (1986) attempted to use Chvorniov's rule to predict the total solidification time for foam casting using bonded sand. He left the process open for further development.

2.7 SEGREGATION

Segregation is one of the problems encountered during solidification of a casting. Segregation is a departure from uniform distribution of the chemical elements in the alloys, Flemings and Brody (1966). The liquids that are frozen to form industrial alloys usually contain in addition to solute elements added intentionally for their useful effects, many impurity elements which are present in the liquid metal by a number of factors. Some of these impurities form nucleation centres for heterogeneous nucleation as solidification proceeds. Because of the way in which solutes in alloys partition between the solid and the liquid during freezing, it allows every casting to be segregated at some extent.

Variation in composition can occur in microscopic scale between dendrite arms and it is known as microsegregation, Clyne and Kurz (1965). Microsegregation can be significantly reduced by homogenization heat treatment because the distance is usually in the range of 10-100µm through which diffusion has to take place for the redistribution of the alloying elements. On the other hand, macrosegregation cannot be removed because it occurs over a large distance in the range, Flemings and Scandinavian (1976) hence impractical to remove by diffusion without geological time scales being available.

2.7.1 PLANAR FRONT SEGREGATION

Usually, there are two main types of normal segregation that occurs when the solid is freezing on a planar front;

i) One that results from the freezing of quiescent liquid and

ii) The other that results from stirred liquid.

Two of them are both important during solidification and give rise to different patterns of segregation. The build up to the steady state condition is called the initial transient. Flemings (1974) shows that for small k (distribution coefficient), the initial transit length is approximately $D/V_S k$.....(18)

Where D is the diffusion coefficient of the solute in the liquid and V_s is the velocity of the solidification front, the subsequent freezing to solid of composition C_O takes place in a steady continuous pattern until the final transient is reached. At this stage, both the liquid and solid phases increase in segregation.

2.7.2 MICROSEGREGATION

As the dendrites grow into the melt and as the secondary arms spread from the main dendrite stem, the solute is rejected, effectively being pushed aside to concentrate in the tiny regions enclosed by the secondary dendrite arms. There is a more or less uniform composition since this region is smaller than the diffusion distance. And this is segregation of solutes at microscopic level. Uniformity of the liquid phase in this case results from diffusion within its small size, rather than any bulk movement of the liquid. The interior of the dendrites therefore has an initial composition close to $kc_{0,}$ Flemings (1974), while towards the end of freezing; the centre of the residual interdendritic liquid has a composition corresponding to the peak of the final transient. Some diffusion of solute in the dendrite will tend to smooth the initial as-cast coring,

and it is called back diffusion. Additional smoothing of the original segregation can occur as a result of other processes such as remelting of secondary arms as the spacing of the arms coarsens.

The partial homogenization resulting from back diffusion and other factors means that, for rapidly diffusing elements such as silicon in aluminium, homogenization is rather effective. The final composition in the dendrite and in the interdendrite liquid is not far from that predicted from the equilibrium phase diagram.

2.7.3 DENDRITIC SEGREGATION

As freezing occurs in the dendrites, the general flow of liquid that is necessary to feed solidification shrinkage in the depths of the pasty or mushy zone carries the progressively concentrating segregates towards the root of the dendrites.

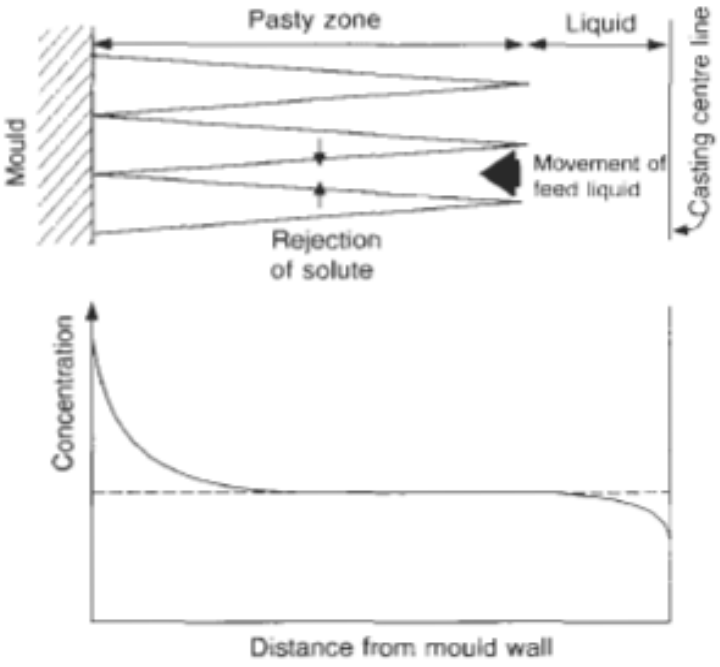

Figure 2.11: Normal dendrite segregation. (Extracted from Campbell, 2003 p143)

The figure above shows normal dendrite segregation or inverse segregation arising as a result of the combined action of solute rejection and shrinkage during solidification in a temperature gradient.

In the case of a freely floating dendrite in the centre of the ingot that eventually form an equiaxed grain, there will be some flow of some concentrated liquid towards the centre of the dendrite if any solidification is occurring at all. For the case of dendritic growth against the wall of the mould, however, the temperature gradient will ensure that all the flow is in direction towards the wall and concentrating the segregation here. Dendritic segregation is observable but it is not usually severe in sand casting due to the relatively low temperature gradients that allow freezing to occur instead of over the cross section of the casting.

2.8 SOLIDIFICATION SHRINKAGE

Shrinkage is a source of crack in the casting or a dishing on the surface of the metal which results from unequal contraction of the metal during solidification. Shrinkage may result from the following

a) Improper location and size of risers, gates and runners
b) Inadequate risers
c) Lack of directional solidification
d) Incorrect metal composition
e) Incorrect pouring temperature

Shrinkage may be eliminated by the use of feeders and chills at proper locations to provide directional solidification of the casting. The molten metal in the furnace considerably occupies more volume than the solidified castings, which are eventually produced giving rise to a number of problems for the founder. There are mainly three different contraction zones in a metal during

solidification from the liquid to room temperature as shown in the figure below.

As the temperature of the liquid metal drops, the first contraction to be noticed is that in the liquid state. The volume of the liquid metal reduces almost exactly linearly with decreasing temperature.

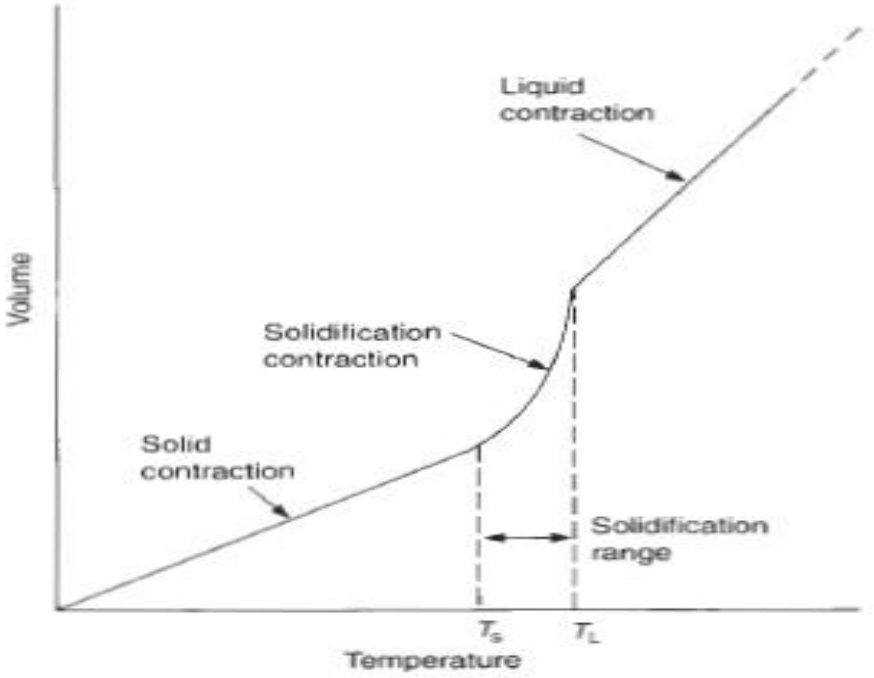

Figure 2.12: Different contraction zones

In casting, shrinkage in the liquid state does not usually poses big challenge to the founder because the extra liquid metal required to compensate for the small reduction in volume is usually provided through gating, runner and risering system without much difficulty.

However, contraction on solidification is quite another problem. This stage of contraction begins at the freezing point of the metal due to the higher density of the liquid when compared to that of the liquid. This zone of contraction leads to other problems such as

i) The requirement for feeding

ii) Shrinkage porosity

The final stage of shrinkage during solidification is the solid contraction which can cause other series of problems. As cooling proceeds, the casting tends to reduce its sizes as a consequence, it meets with a constraint to some extent which could be mould wall or even the other parts of the casting which has solidified and cooled already. These constraints always lead the casting to be somewhat larger than the mould is expected from free contraction alone and hence the pattern is made over size to accommodate for shrinkage allowance.

In general, the liquid metals contract on freezing because of the arrangement of atoms from an open random closed-packed arrangement to a regular crystalline array of significantly denser packing. The densed solid are those that have cubic closed packed. Example: face centred cubic (fcc), hexagonal closed pack (hcp), etc. There are materials that expand on freezing. They may include water, silicon, bismuth, etc.

2.8.1 UNIFORM CONTRACTION

The contraction of a casting from its freezing temperature to room temperature always poses great challenge to the pattern maker. This is because the pattern must be designed over size by amount known as the contraction allowance so that the casting will fit at the correct size at room temperature. The greatest problem to the pattern designer is to determine the exact amount of the allowance during designing of the pattern. The different contractions are the results of different degrees of constraints by the mould during cooling. For example, for the case of zero constraint casting, such as straight bar will contract freely to its maximum extent without obstruction. But for high mould constraint, the contraction will meet resistance from the mould wall and as a result will not contract freely.

2.8.2 NON-UNIFORM CONSTRAINT OR DISTORTION

In an ideal situations where the castings were to be cooled at uniform rate with uniform constraint acting at all points over its surface, then it will reach room temperature perfectly in proportion; maybe a little larger or a little small, but not disturbed. But in real practical situation, this assertion is non realisable. Usually the casting is either larger or smaller and dose not poses the accurate shape it was designed to be. Occasionally the casting may be seriously distorted. Two major sources of the distortions are

a) Mould constraint

b) Casting constraint

2.8.3 INITIATION OF SHRINKAGE POROSITY

Considering a perfect condition where there is no gas and if feeding is adequate then no porosity would be found in the casting. Unfortunately, however, in the real practical situation, many casting are sufficiently complex that one or two regions of the casting are not adequately fed. With the result that the internal hydrostatic tension will increase, reaching the level at which internal pores may form in different ways. Conversely, if the internal tension is kept well by effective solid feeding, the mechanisms for internal pores formation are not triggered. The solidification shrinkage appears on the outside of the casting.

If the pressure inside the casting falls, then the liquid that is still connected to the outside surface maybe drawn from the surface, causing the growth of porosity connected to the surface. The sucking of liquid from the surface in this way naturally draws in air through intedendritic channels, spreading along the routes into the interior of the casting. This phenomenon is a type of feeding by a fluid, where the fluid in this case is air. The porosity in

the interior of the casting cannot be differentiated from micro porosity caused by other ways. In alloy of intermediate freezing range, the initiation site is usually hot spot such as an internal corner or re-entrain angle.

Short freezing range alloys such as Al-Si eutectic, do not usually exhibit surface-connected porosity. They form a sound solid surface skin at an early stage of freezing and liquid freezing continues undisturbed through wide open channels. Any final covering of internal pressure due to poor feeding towards the end of freezing may then create a pore by nucleation in the interior liquid. Here, there is no connection to the outside surface of the casting, after nucleation, further solidification will provide the driving force for growth of the pore. Therefore is alloys of short freezing rage, porosity is probably normally nucleated and is always concentrated at the centre of the casting.

2.8.4 GROWTH OF SHRINKAGE PORES

The initial growth of the internal pores that are nucleated within the stressed liquid is extremely fast. It is rather explosive. The elastic stress in the liquid and the surrounding solid can be dissipated at the speed of sound. The tensile failure of liquid is similar to the tensile failure of a strong solid. It gives a loud reaction. After the explosive growth phase, the subsequent growth of the pore was more leisurely, occurring at a rate assumed to be controlled by the rate of solidification. In other words, we can conclude that the second phase of growth is controlled by the rate of heat extraction by the mould.

The pores that are initiated at surface have lower initial stress and the puncture of the surface will occur relatively slowly as the surface collapses plastically into the forming holes. For shrinkage porosity that grows like a pipe from the free surface of the melt, there is no initial fast growth present, Davies (1963). The cavities grow at all stages simply in response to the solidification

shrinkage. The rate is determined by the rate of heat extraction from the casting.

2.9 MOULD AND METAL GAS REACTION

This section has to do with the reactions occurring between the gases within the melt and mould wall at the solid/liquid interface.

2.9.1 GASEOUS INTERACTIONS WITH THE MELT

Liquid metal is a highly reactive chemical. Metal is capable of reacting with the gases above it, the solid material of the crucible which contain it and even with the mould walls during casting. Liquid metal is highly reactive that is can also react with any type of slag or even flux floating on top of the melt. Sometimes the reactions between the liquid metal and ions that are in contact can be explosive; hence liquid metal has to be handled carefully. The melt tends to attain equilibrium state and this is the driving force for the high reactivity of liquid metals. They are highly unstable at liquid state and as a result have high entropy. The progression to equilibrium state is limited by the rate at which reactions take place and the available time. The reactions in the crucible or the furnace during melting of a metal are seen to be serious because there is usually plenty of time for extensive changes. Liquid metals usually pick-up hydrogen from damp refractoriness. It is also common with metals which are melted in furnaces heated by burning of hydrocarbon fuels. For example gases or oils. If the chemical composition of hydrocarbon is denoted C_XH_y respectively straight chain compounds such as methane CH_4, ethane C_2H_6 etc or aromatic group such as benzene C_6H_6, etc, the equation for the combustion of fuel such as methane can be written as

$$CH_4 + 2O_2 \rightarrow CO_2 + H_2O \quad \text{.....(19)}$$

The hot waste gases from such furnaces are effectively wet. The moisture from linings or atmosphere can react with the liquid metal, M.

$M + H_2O \rightarrow MO + H_2$.....(20)

Thus, a little metal is scarified to form oxide and the hydrogen is released to equibrate itself between the gas and the metal phases. In the case of some aluminium alloys, the sacrificial lost of metal is minimized by the formation of protective thin film oxide layer. Solubility of hydrogen in aluminium increases with an increased in temperature.

2.9.2 ALUMINIUM ALLOYS AND GASES

If we consider first the reaction of aluminium with oxygen, the solubility of oxygen in aluminium is extremely low, less than that of about one atom in about 10^{35}atoms. The solubility of aluminium can be approximated to zero, yet we all know that aluminium and its alloys are full of oxides. The oxides certainly cannot have been precipitated by reaction with oxygen in solution. The oxygen can only react with the surface and the surface can only access the interior of the metal if it is entrained or folded in. The process of aluminium oxide formations is more of mechanical process rather chemical process.

The reaction of hydrogen in aluminium is much different from that of oxygen with aluminium. The solubility of hydrogen in liquid aluminium is illustrated in the diagram below.

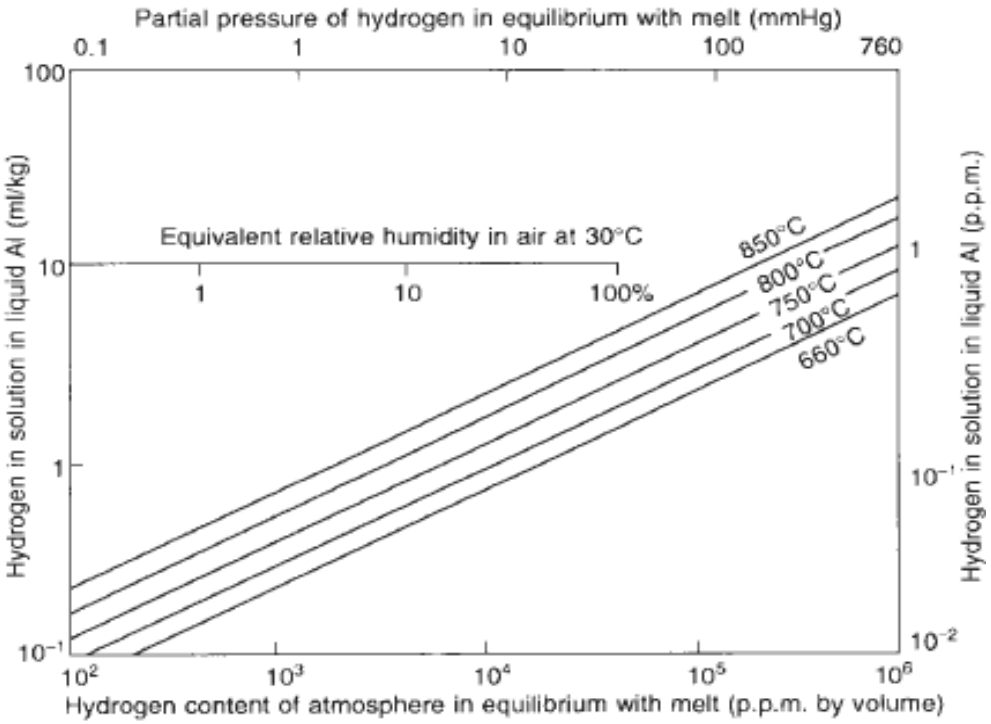

Figure 2.13: Hydrogen content of liquid aluminium shown as increasing with temperature

Low gas content is only attained under conditions of a low partial pressure of hydrogen. This shows that hydrogen is more soluble in liquid aluminium than oxygen.

2.9.3 TRANSPORT OF GASES IN MELTS

Gases in liquids travel most quickly when the liquid is moving since they are simply carried by the liquid under convection heat transfer. But in many cases of interest, the liquid is stationary or stagnant. This is the situation found in the boundary layer at the surface of the liquid. The existence of solid film on the surface will make the surface stationary and due to the effect of viscosity, the stationary region will extend to some distance into the bulk liquid. Within stagnant liquid of the boundary layer, the movement of solutes can occur only by the slow process of diffusion instead of fast movement by fluid convection. Another region where diffusion is important is the partially solidified zone or

the mushy in the zone of the solidifying casting, where the flow of fluid is usually slow. In the solid state, diffusion is the only mechanism by which solutes can spread. In solid, there are two major types of diffusion movement of atoms viz interstitial diffusion of atoms and substitution diffusion movement of atoms. Hydrogen is a gas that can diffuse interstitially as a result of its small size. Common alloying elements of aluminium such as Mg and Cu clearly show substitution solute diffusion movement.

2.10 DEFECTS OF CASTING

The defects in a casting can be as a result of pattern and moulding box equipment, moulding sand, cores and gating systems or molten metal. The production of sand castings is of great importance economically. Design and practice are of importance in influencing the incidence of casting defect. Most often, error are made in design and can be compensated for by the applications of operations involving the careful control of the cast metal and that of the3 casting procedure.

Some of the defects in casting and their reasons are

2.10.1 MOULD SHIFT

Mould shift is a casting defect that results in a mismatching of the top and bottom parts of the casting. It usually occurs at the parting line. Mould shift is caused by

i) Misalignment of pattern parts due to worn out or damage patterns.

ii) Misalignment of moulding box or flask equipment. Mould shift can be prevented by proper alignment of the pattern, moulding boxes, correct moulding of pattern on pattern plates, replacement of worn out patterns etc.

2.10.2 CORE SHIFT

Core shift is an abnormal variation in dimensions which are dependent on core position. Core shift can be caused by

i) Misalignment of cores in assembling cored-moulds

ii) Undersized and oversized core prints

iii) By using incorrect size of chaplet

This defect can be remedied by providing the core at the proper place and must be gripped firmly in the sand. Also correct size of the core prints must be used.

2.10.3 SWELL

Swell is an enlargement of the mould cavity by the pressure of the molten metal resulting in localised or general enlargement of the casting. When swell occur, the dimensions of the casting will be bigger than what was initially designed for. Swell can be caused by one of the following reasons:

i) Insufficient ramming of the sand

ii) Insufficient weighting of the mould during casting.

iii) Pouring of the molten metal too rapidly or too hard

2.10.4 FINS AND FLASH

Fins and flash are thin projections of metal not designed for as a part of casting. These defects usually occur at the parting line of the mould or core sections. This may be caused by

i) Excessive ramming of the pattern before it is rewritten from the mould.

ii) Insufficient weight on the top part of the mould.

iii) Loose champing of the mould.

2.10.5 SAND WASH

Sand wash is the type of defect that is caused by the erosion of the mould wall by the molten metal. It usually occurs near the ingates as rough lumps on the surface of casting. The sand that has been washed away appears on the upper surfaces of the casting as rough holes or depressions. Sand wash may be due to the following reasons

i) Soft ramming of sand

ii) Weak sand

iii) Poor pattern design and construction

iv) Insufficient draft allowance

Sand wash is majorly avoided by proper ramming of sand.

2.10.6 HOT TEAR

Hot tear is an internal or external ragged discontinuity in the metal casting resulting from hindered construction occurring just after the metal has solidified. This defect can be caused by the following reasoned

i) Abrupt changes in section, inadequate filleting of inside sharp corners, and improper positioning of chills

ii) Poor collapsibility of mould and core materials which will place extra stress on certain details.

iii) Improper pouring temperature.

2.10.7 BLOW HOLE OR SAND BLOW

Blow hole is a common defect encountered in sand casting. It is extremely smooth depression on the outer surface of a casting. Blow hole is caused by

i) High moisture content in moulding sand.

ii) Low permeability of sand.

iii) Hard ramming of sand.

iv) Poor gating system design.

v) Improper venting of sand.

This defect can be avoided by completing drying up the mould, proper venting, selecting sand with the required permeability and good in-gate system for the flow of molten metal.

2.10.8 CORE BLOW

Core blow is an excessive smooth depression on the inner surface of a cored cavity. Core blow is caused by using insufficient baked cores. Thus to remedy this defect, the core should be sufficiently baked before using in casting.

2.10.9 SLAG HOLES

This defect is also called honey combing. They are smooth depressions on the upper surfaces of the casting. They usually occur near the in gates. Slag holes are due to improper skimming of the metal or due to poor metal. They can be avoided by preventing the slag from entering along the molten metal.

2.10.10 SCAB

Scabs are pattern or slightly raised area of sand on the upper surface of the casting. They are caused by

i) Uneven ramming of sand.

ii) Slow or intermittent running of liquid metal.

Proper ramming of sand and uniform flow of the molten metal into the mould can prevent this defect. Another way of avoiding scab is to mix additions such as wood floor, sea coal or dextrin to the moulding sand.

2.10.11 MISRUNS AND COLD SHUTS

These defects occur when the mould cavity is not completely filled and incomplete castings results. Misruns are caused by

i) Two small gates.

ii) Too many restrictions in the gating system.

iii) If pouring head is too low.

iv) Faulty venting of the mould.

v) Metal lack in fluidity.

In order to eliminate these defects, the casting should be designed keeping in mind the fundamental principles of gating and rising. The thin sections should be preheated and the molten metal should be poured at the appropriate temperature.

2.10.12 POUR SHORT

This defect occurs when the mould casting is not completely filled because of insufficient metal. It is caused by the following reasons

i) Interruptions during pouring operation

ii) Insufficient metal in the ladles being used to pour the molten metal.

To avoid pour short, the ladles should have sufficient molten metal at the correct temperature.

2.10.13 METAL PENETRATION

This type of defect occurs when the alloys being cast tend to penetrate into the sand grains and cause a fused aggregate of metal and sand on the surface of the casting. It is due to the following reasons

i) Soft rammed sand

ii) Moulding sand and core sound being too coarse

iii) Improper use of mould and core washes will cause penetration

iv) Excessive metal temperature or increased fluidity of metal.

2.10.14 ROUGH SURFACE FINISH

Rough surface finish is a defect characteristic by merely a lack of sufficient smoothness in the casting. It is caused by the following

i) Soft ramming of sand

ii) Coarse sand

iii) Hard pouring or too high metal fluidity

iv) Improper use of mould and core washes often promotes rough surface casting.

This can be avoided by using a proper mould and ramming of sand.

2.10.15 RUN-OUT AND BUST-OUTS

These permit drainage of the metal from the casting and result in incomplete casting. They are caused by

A. A pattern that is too large for a given flask or pattern placed too close to the flask edge resulting in a weak spot and cause run-out

B. The match plate surfaces that are out of parallel or uneven results in a poorly formed parting line and cause run-out.

C. Improper sealing of mould joints causes run-outs.

D. Inadequate weight or clamps will permit the cope to lift which results to a run-out.

E. Excessive pouring pressures may cause this defect

F. Malalighnment of cope and drag many promote run-out.

CHAPTER THREE

MATERIALS AND EXPERIMENTAL PROCEDURE

3.1 MATERIALS

3.1.1 Aluminium, Al

Aluminium is the parent material of the alloy produced from the casting up to 92.6% by composition. Scrap aluminium profiles and lumps were sourced from First Aluminium in Port Harcourt and aluminium roofing companies (Vinal Aluminium and Max Aluminium) here in Owerri.

3.1.2 Silicon, Si

Silicon was the first alloying element used during the casting of this Al-Si-Mg system. It contained Silicon in excess of 5.43%Si. The silicon was sourced from Metallurgical Training Institute, Onitsha, Anambra State in the form of fine black powders.

3.1.3 Magnesium, Mg

Magnesium was the second alloying element in this aluminium alloy system. It was sourced from the chemical market at Head Bridge in Onitsha, Anambra State in the form of lumps.

3.1.4 Sodium, Na

Sodium was introduced into the system during the casting of the alloy as a modifying agent for the solidified structures. It was obtained in the form of white lumps that were stored under parafin oil due to its high reactivity in the atmosphere. It was sourced from the chemical market at Onitsha Head Bridge.

3.1.5 Strontium, Sr

Strontium is another modifying agent that was used during the casting of the alloy. It was in the form of white powder. Strontium was sourced from chemical market at Onitsha Head Bridge.

3.1.6 Charcoal

Lumps of charcoal were used to provide heat that was used to melt the aluminium and the alloying and modifying elements.

3.1.7 Phenolic Powder

A greenish phenolic powder was used for the mounting of the samples for microstructural analyses. The powder was obtained from laboratory of Materials and Metallurgical Engineering Department of Federal University of Technology, Owerri.

3.1.8 Sand Papers

Sand papers of different grades were used to grinding the surfaces of samples after mounting operation. Sand Papers were obtained from new market in Owerri.

3.1.9 Diamond Liquid

It is a liquid that was used on the emery cloth during the polishing of the samples on the polishing wheels. It was obtained in Materials and Metallurgical Engineering laboratory.

3.1.10 Hydrogen Fluoride

Hydrogen fluoride is the chemical/acid that was used for etching the surface of the samples to reveal the microstructure when examined with the

metallurgical microscope and was obtained from the same Materials and Metallurgical Engineering laboratory.

3.2 EXPERIMENTAL PROCEDURE AND METHODS

The experimental procedure of this work consists of

i. Pattern making
ii. Moulding
iii. Melting and casting
iv. Tensile testing
v. Microstructure examination

The first section was the production of samples for examinations. The production was done using sand casting process. In the second part, tensile test of the samples produced was worked on to check the effect of different cooling rates and modification on the structures. The third section of this work which does not require specimen preparation dwell on the hardness properties of the samples. And lastly the fourth section described and examined the internal structures of the different samples produced.

3.2.1 CASTING

Alloying and modifications of the Al-Si-Mg system was done by sand casting process. Casting operation was carried out at the foundry workshop of Federal University of Technology, Owerri under the supervision of foundry technologist. This metal casting operation consists of various steps that lead to the production of the sand casting. Three different castings were produced, with unmodified, Na modified and Sr modified but same compositions of the alloying elements. The following steps were taken to produce the alloy;

3.2.1.1 WEIGHING

Weighing of the various elements that was used during the casting operation was carried out in the Agricultural Engineering laboratory section of workshop II of Federal University of Technology Owerri using standard weighing balance. Weighing was done to maintain consistency in mass and composition of the alloying elements and modifiers in the alloying system. 630g of Al was measured into three places, 37.7g Si measured into three places and 26.6g of Mg also measured at three places because three different castings with uniform composition were produced. Again 7.6g of sodium and 10.06g strontium were measured during the casting with portable digital hand weighing balance. This sodium and strontium were used in separate castings as modifiers and the remaining casting was unmodified.

3.2.1.2 PREPARATION OF PATTERN AND MOULD

Cylindrical pattern made of steel was used for the castings. Because of the need to check the effect of different cooling rates, the cylindrical steel pattern was designed to have five different sections of different thicknesses. The different thicknesses in dimension will ensure different cooling rates for each section with the largest section having the slowest cooling rate and the smallest section with the fastest cooling rate.

A mould was built around the pattern with already constructed wooden box. The pattern was placed inside the cope of the wooden box and filled and rammed with the moulding sand. Moulding powder was sprinkled on the cope and the drag section of the mould introduced. Sand blower was used to blow the surface between the cape and the drag. A riser was carefully made with a round pipe by pressing it through the section of the mould.

3.2.1.3 CHARGING AND MELTING

Three different castings with each casting having five sections that cooled differently were produced. In each casting, 630g of aluminium scrap was charged in a crucible furnace in the foundry workshop of Federal University of Technology Owerri. Charcoal was used to produce the heat required to fire the system to the melting temperature. The crucible containing the aluminium was placed on top, and the manual blower that was constantly rotated, thereby rekindling the heat from charcoal used for melting. The melting was enabled with the large amount of heat from the charcoal. In each case the melting of aluminium took between 50 to 60 minutes before the aluminium was completely melted.

3.2.1.4 ALLOYING, TEMPERATURE MEASUREMENT AND POURING

When the aluminium was completely melted, the alloying elements were introduced. Silicon was introduced in the form of powder into the liquid aluminium; hence we have large surfaces for reactions which will make the alloying more easily. Earlier the magnesium were been introduced during the unset of aluminium melting.

A thermocouple device was used to measure the various temperature changes. The first liquid formed at 660^0C. As the firing continued more liquid formed until the whole aluminium scrap turned to liquid aluminium. Higher temperatures of 690^0C, 708^0C, 750^0C were obtained and the temperature peaked at 814^0C with a very high fluidity.

After the alloying and peak temperature attained, the temperature was allowed to drop below 790^0C prior to the modification by Na and Sr and subsequently pouring. Modification was done at lower temperature than alloying in order to ensure high rate of recovery of modifiers. The modifiers,

sodium and strontium are very reactive and may vaporize at higher temperature and prolonged time; hence the temperature must be reduced before modification. Pouring of the alloy is done immediately after the modification and at lower temperature. Another good reason the peak temperature was allowed to drop before pouring is to avoid tendency of hot cracking. Aluminium is susceptible to hot cracking and hence, the pouring must not be carried out at peak temperature of 814^0C.

3.2.2 TENSILE TEST AND PROCEDURE

Tensile test as a mechanical test is used to study the effect of different cooling rates on brittleness and ductility of this particular alloy. It also aimed to see if there is any effect of modifications on the mechanical properties of the alloy. The tensile test was conducted at the Materials and Metallurgical Engineering laboratory section of workshop II in FUTO. A tensometer for tensile test was used.

3.2.2.1 SPECIMEN PREPARATION

Each of the castings produces five specimens with different dimensions for various tests. Three different castings were produced giving a total of 15 specimens. For this tensile test, a lathe machine was used for the specimen preparation. The materials were prepared round by reducing the cross sectional areas to have a uniform dimensions confirming to the standard specification of the tensile test specimen. The dimensions where reduced to 5mm diameter and gauge length of 28mm using lathe machine.

3.2.2.2 TEST

The test was done using tensometer. The material for testing was fixed with a pair of chucks and the set up was fixed to the tensometer. Load was applied until the material fractured. With the cursor, the graph was traced with a standard graph sheet for tensile test. The material was removed, with the use of calliper, the final length l_f and final diameter d_f were measured.

3.2.3 HARDNESS TEST

Hardness testing does not require specimen preparation; hence it is a straight forward test. The hardness test was also carried out in the same laboratory as the tensile test. A Rockwell hardness testing machine was used. 15kg minimum load was used. Rockwell B working load of 100kg was used. The material was scratched until indentation was made on the surface of the material and the results were read from the die or the Rockwell B scale.

3.2.4 MICROSTRUCTURE EXAMINATION

Metallurgical microscope was used to observe the effect of cooling rate on the internal structure of the alloy. The test was carried out in the Materials and Metallurgical Engineering laboratory. The steps and procedures for the micro structural analysis are given below

3.2.4.1 SPECIMEN PREPARATION AND MOULDING

The 15 specimens for microstructure analysis were cut and machined using hacksaw, vice and lathe machine. After the samples were prepared, they were mounted using a mounting pressing machine. The mounting operation was done in the laboratory of Material and Metallurgical Engineering. The samples were mounted into phenolic powder, with the application of force and

heat, the powder set into a solid. The phenol powder is a thermosetting material.

3.2.4.2 GRINDING

After mounting the samples, they were ground to reveal more interior part of the internal structure. Different grades of sand papers were used to reduce asperities on the surface of the materials until a mirror like surface was obtained. The grades of the sand papers that were used are P220C, P320C, P400C, P600C, P800C and p1000c. These papers are called abrasive paper or silicon carbide paper. The grinding started with abrasives with coarser particles to the abrasives with the finest surface because it will help to reduce the asperities to the barest minimum and produce a mirror- like surface.

3.2.4.3 POLISHING

The next operation after grinding is polishing. The surface was polished to further reduce asperities (risers and valleys) and scratches from the surface of the specimen in order to obtain a clearer and smoother surface. Polishing was enabled with the use of diamond liquid sprinkled at the surface of emery cloth.

3.2.4.4 ETCHING AND VIEWING

After the samples have been precisely polished, the surfaces were etched with a hydrogen fluoride acid to reveal the microstructure, photomicrographs were obtained with the aid of a camera attached to a metallurgical microscope at magnification of X100 and X400.

CHAPTER FOUR

RESULTS AND DISCUSSION

4.1 COOLING CURVES

Three different castings were produced. One was strontium modified, another one was sodium modified and the last casting was unmodified. They all have the same composition except for the modifications. Each casting has five different sections that cooled differently. In order words five samples were obtained from each cast alloy.

The cooling curves obtained in this section for the Al-Si-Mg alloys are due to different cooling rates as a result of variation in the section thicknesses of the castings produced. Since the same mould material was used for all the castings, the different cooling rates cannot be explained using heat diffusivities of mould material. Therefore, the total solidification times and cooling rates obtained from cooling curves can be linked to the section thickness (dimensions).

It is widely expected that the five sections of each casting produced will give different cooling rates and subsequently different cooling curves. Thermocouple and stop watch were successfully used to monitor the cooling rates from which the cooling curves were developed. The cooling curves for the Al-Si-Mg alloy in the five different dimensions are shown in the figures below. In each section, the curves for different cast thicknesses are shown. It can be shown that the casting thickness with the smallest dimension has the fastest cooling rate and hence relatively shortest solidification times.

Table 4.1: Cooling Temperatures and Times for all the Sections

Temp (^{0}C)	**Time (s)**	**Time (s)**	**Time (s)**	**Time (s)**	**Time (s)**
	5mm x 50mm	**10mm x 50mm**	**20mm x 50mm**	**30mm x 50mm**	**40mm x 50mm**
28	5	7	8	8	11
750	11	14	18	24	29
650	35	58	78	95	111
550	135	179	211	245	270
450	220	280	321	374	425
350	338	410	475	520	565
250	580	645	705	780	855
200	770	860	950	1040	1150

4.1.1 COOLING CURVE I (5mm x 50mm)

This is the part of the casting that has smallest thickness dimension for all the casting composition, that is Na modified, Sr modified and unmodified castings. As a result, it has the shortest possible total solidification and fastest cooling rate which is made manifest in its cooling curve.

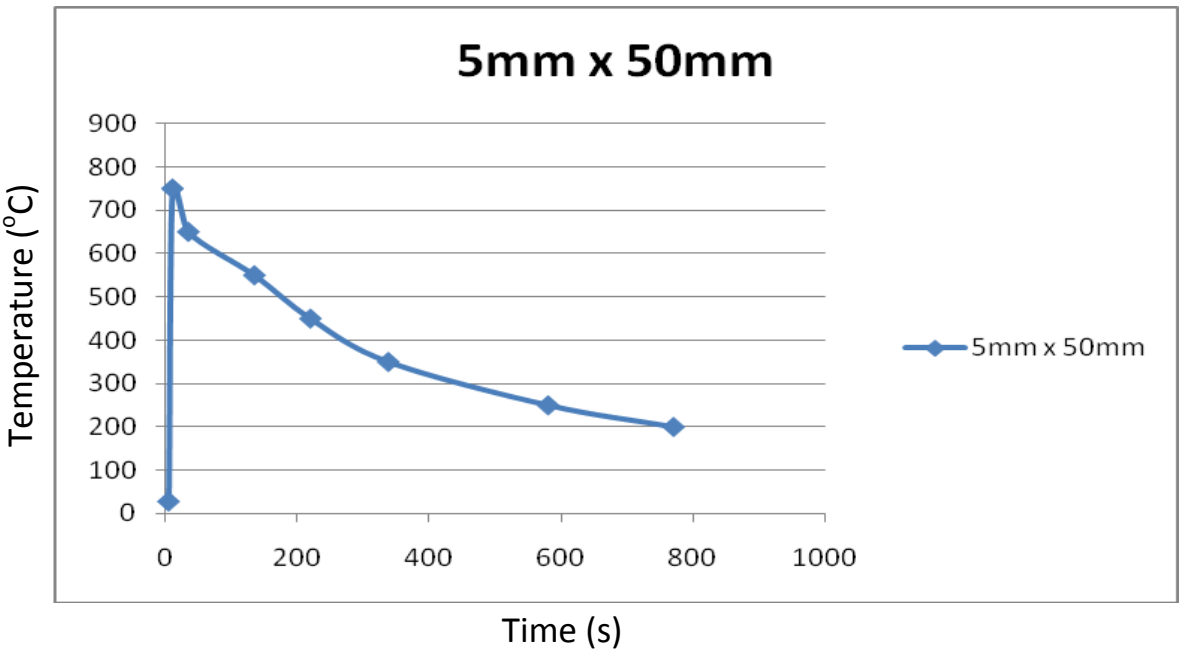

Figure 4.1: Cooling curve I (5mm x 50mm)

4.1.2 COOLING CURVE II

As the section thickness increased from 5mm x 50mm to 10mm x 50mm, there is a noticeable change in the cooling rate which is also represented in the cooling curve in the figure below. It took more time for this section to cool from 766^0C to 630^0C than it took the previous section

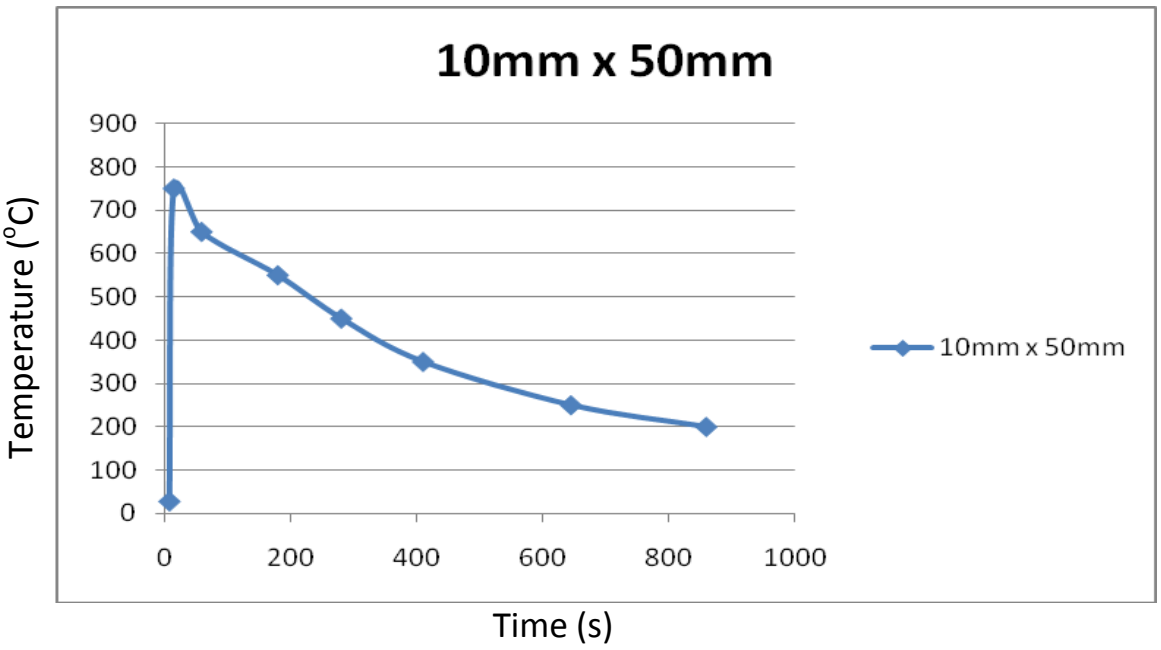

Figure 4.2: Cooling curve II (10mm x50mm)

4.1.3 COOLING CURVE III

As the section thickness continued to increase, at 20mm x 50mm thickness, the cooling rate continued to reduce which consequently lead to increase in total solidification time.

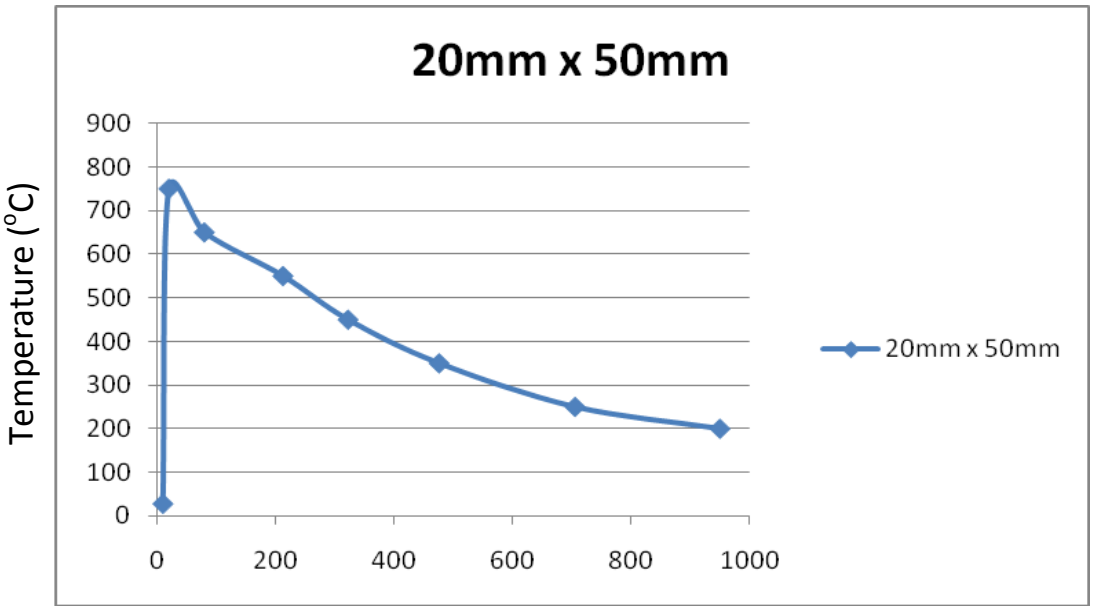

Figure 4.3 Cooling curve III (20mm x30mm)

4.1.4 COOLING CURVE 1V

On further increments on the section thickness, the time of solidification continued to increase further, which causes slight deviation of their cooling curves. Local and total solidification times continued to build up.

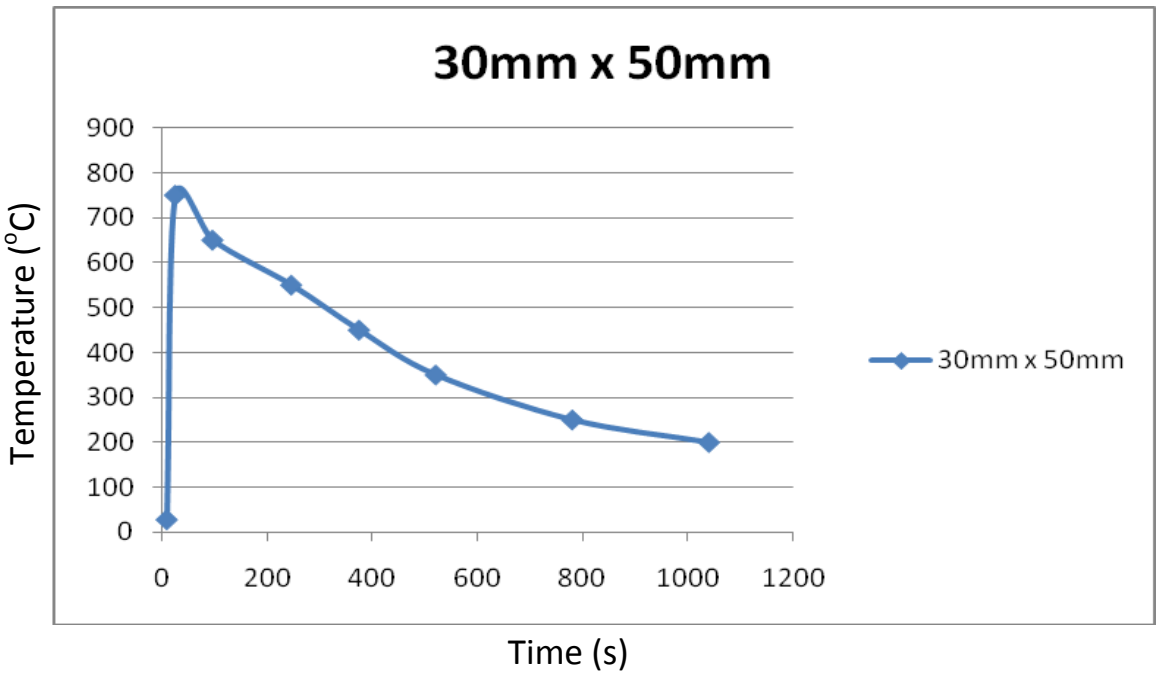

Figure 4.4: Cooling curve IV (30mm x 50mm)

4.1.5 COOLING CURVE V

The section that has 40mm x 50mm is the biggest section of the casting the highest possible solidification time. The cooling rate is slowest at this part of the alloy. This change in cooling rate continued to cause consistent change in their cooling curves.

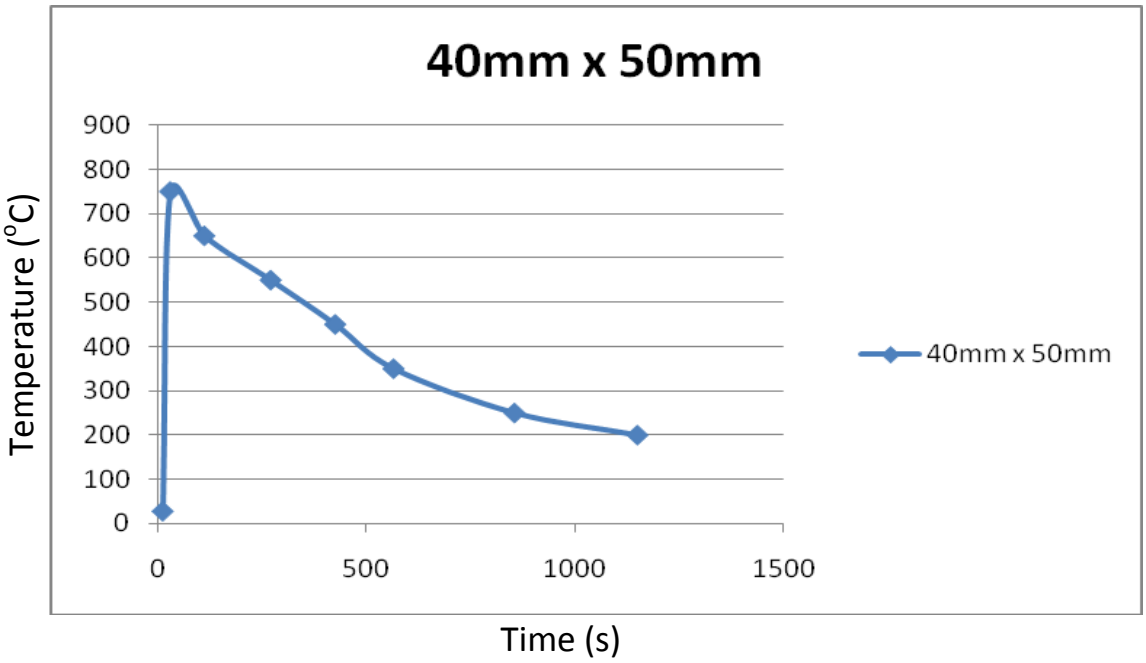

Figure 4.5: Cooling curve V (40mm x 50mm)

When you combine the five graphs together, it will give a clearer difference of their cooling rates.

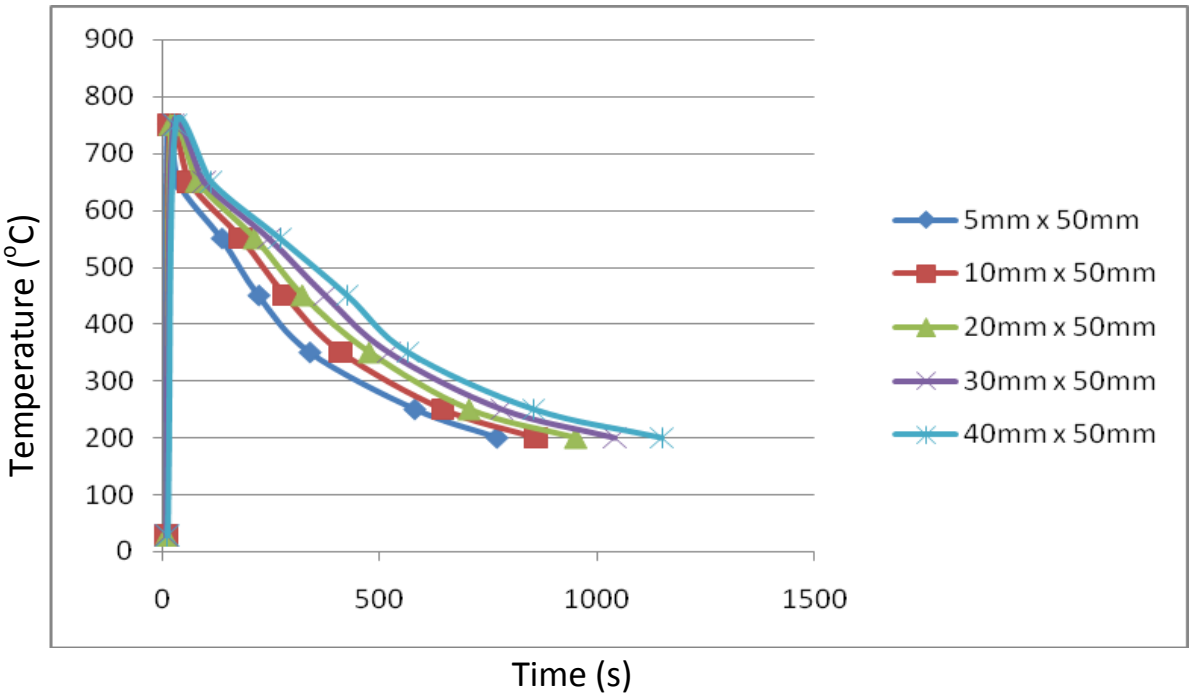

Figure 4.6: Combined curves for all the sections

4.2 TENSILE PROPERTIES

Al-Si-Mg alloy was used in this research and all the three castings have the same compositions. It was observed that cooling rate is proportional to heat extraction from the specimen during solidification. At low cooling rate (in the section with biggest thickness), the rate of heat extraction from the samples was slower and that is evident in cooling curve that is large as shown in figure for cooling curves in section 4.1 above. At higher cooling rate (for those in smaller section), it was observed that the rate of heat extraction from the samples was faster, this can also be revealed in stress-strain curves of the tensile test data below. The slopes are steeper for faster cooling rates because they poses higher tensile strength and smaller ductility. The slow cooling rates are more ductile and have smaller slopes because of more elongation.

It was observed that cooling rates have considerable effect on the aluminium alloy nucleation temperatures. It was noticed that aluminium to nucleation temperature increases with increasing cooling rates from the large sections to the smaller ones. Because of increase in cooling rate, nucleation undercooling increases. Clusters on of atoms form earlier at higher cooling rate than at slow cooling rate and this has effect on the grain size of the casting which in turn improves the mechanical properties of the of the samples produced.

Tensile properties of aluminium alloys have been found to strongly depend on cooling rates. This is shown in various graphs produced for each section of the three cast samples. Increasing the cooling rate greatly reduces secondary dendrite arm spacing (SDAS) as can be seen in the microstructure in subsequent section. Tensile properties increase with a decrease in SDAS. From this work, small sections have lower SDAS. The tensile test curves can be used to explain this further. For example, in the unmodified sample produced, the

section that has the highest cooling rate is 5mm x 50mm casting while the one that has slowest cooling rate is 40mm x 50mm section. Comparing their UTS from their stress strain graphs, it is evident that the section with faster cooling rate has bigger UTS of 112 N/mm^2 while the modulus with slower cooling rate has lower UTS of 81.5 N/mm^2.

4.2.1 UNMODIFIED TEST RESULTS

Table 4.2: Unmodified 5mm x 50mm sample

(N) Load	(mm) Ext.	(mm) L_o	(mm) D_o	(mm) D_f	$(mm)^2$ A_o	(N/mm^2) Stress	$(x1o^{-3})$ Strain	(HRB) Hardness
0	0.000	28	5	4.710	19.642	0.000	0.000	51.500
400	0.125	28	5	4.710	19.642	20.365	4.464	51.500
1000	0.363	28	5	4.710	19.642	50.911	12.964	51.500
1500	0.625	28	5	4.710	19.642	76.367	22.321	51.500
1800	0.750	28	5	4.710	19.642	91.640	26.786	51.500
2000	0.844	28	5	4.710	19.642	101.823	30.143	51.500
2100	1.188	28	5	4.710	19.642	106.914	42.427	51.500

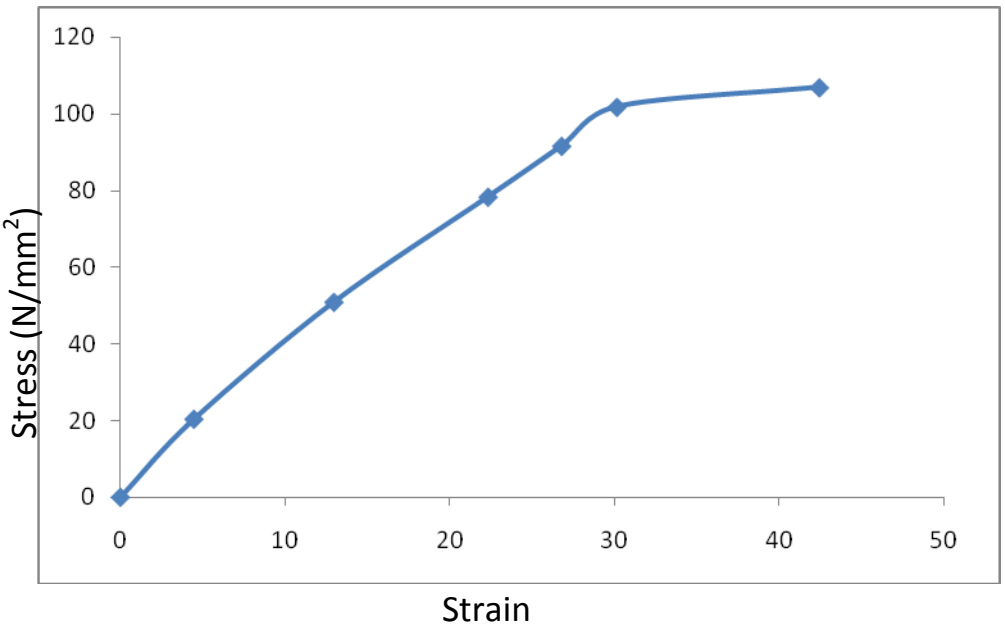

Figure 4.7: Stress-Strain curve for unmodified 5mm x50mm

Table 4.3: Unmodified 10mm x 5omm sample

(N) Load	(mm) Ext.	(mm) L_o	(mm) D_o	(mm) D_f	$(mm)^2$ A_o	(N/mm^2) Stress	$(x1o^{-3})$ Strain	(HRB) Hardness
0	0.000	28	5	4.650	19.642	0.000	0.000	56
400	0.188	28	5	4.650	19.642	20.365	6.714	56
800	0.375	28	5	4.650	19.642	40.729	13.393	56
1300	0.625	28	5	4.650	19.642	66.185	22.321	56
1600	0.813	28	5	4.650	19.642	81.458	29.036	56
1800	1.000	28	5	4.650	19.642	91.640	35.714	56
2000	1.250	28	5	4.650	19.642	101.823	44.643	56

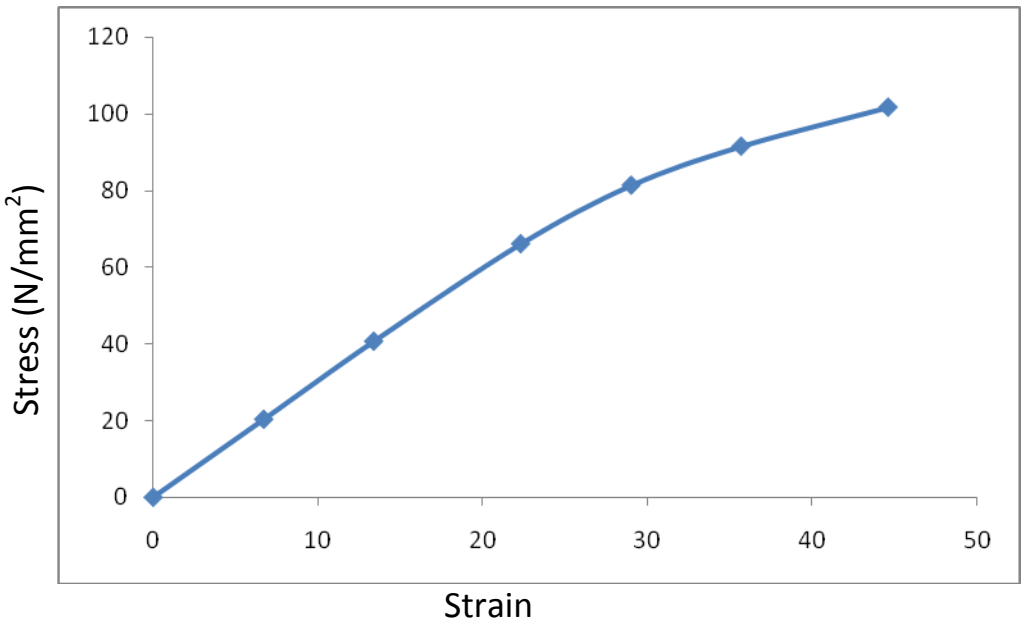

Figure 4.8: Stress-Strain curve for unmodified 10mm x50mm

Table 4.4: Unmodified 20mm x 50mm sample

(N) Load	(mm) Ext.	(mm) L_o	(mm) D_o	(mm) D_f	$(mm)^2$ A_o	(N/mm^2) Stress	$(x1o^{-3})$ Strain	(HRB) Hardness
0	0.000	28	5	4.550	19.642	0.000	0.000	60
400	0.144	28	5	4.550	19.642	20.365	5.143	60
800	0.375	28	5	4.550	19.642	40.729	13.313	60
1200	0.625	28	5	4.550	19.642	61.094	22.321	60
1600	1.063	28	5	4.550	19.642	81.458	37.964	60
1800	1.250	28	5	4.550	19.642	91.640	44.643	60
1700	1.425	28	5	4.550	19.642	86.549	50.893	60

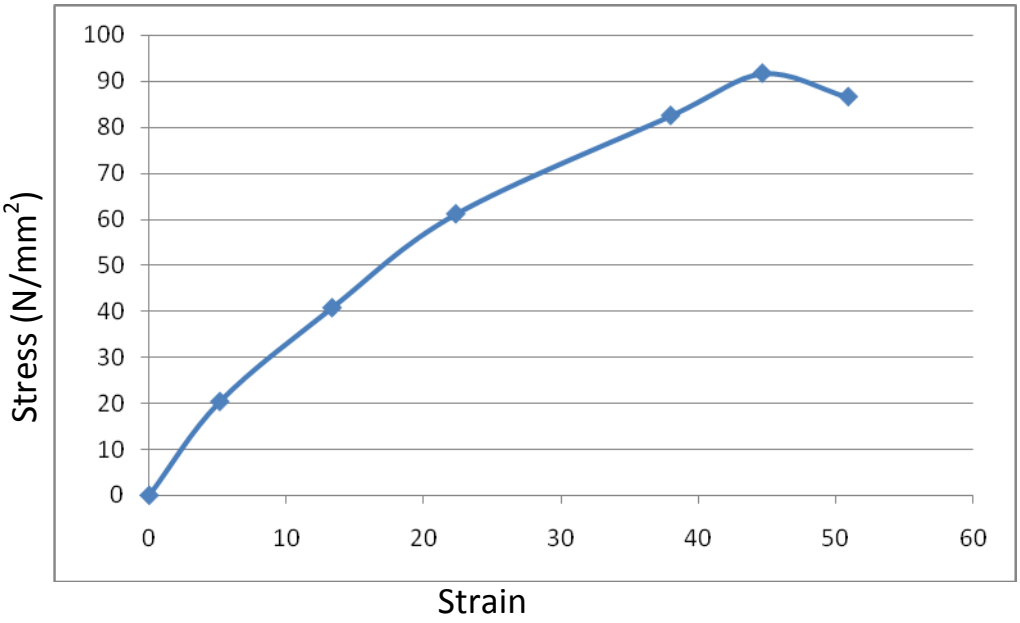

Figure 4.9: Stress-Strain curve for unmodified 20mm x50mm

Table 4.5: Unmodified 30mm x 50mm sample

(N) Load	(mm) Ext.	(mm) L_o	(mm) D_o	(mm) D_f	$(mm)^2$ A_o	(N/mm^2) Stress	$(x1o^{-3})$ Strain	(HRB) Hardness
0	0.000	28	5	4.400	19.642	0.000	0.000	61
400	0.188	28	5	4.400	19.642	20.365	6.714	61
800	0.444	28	5	4.400	19.642	40.729	15.857	61
1100	0.625	28	5	4.400	19.642	56.002	22.321	61
1400	0.919	28	5	4.400	19.642	71.276	32.821	61
1600	1.250	28	5	4.400	19.642	81.458	44.643	61
1500	1.375	28	5	4.400	19.642	76.367	49.107	61

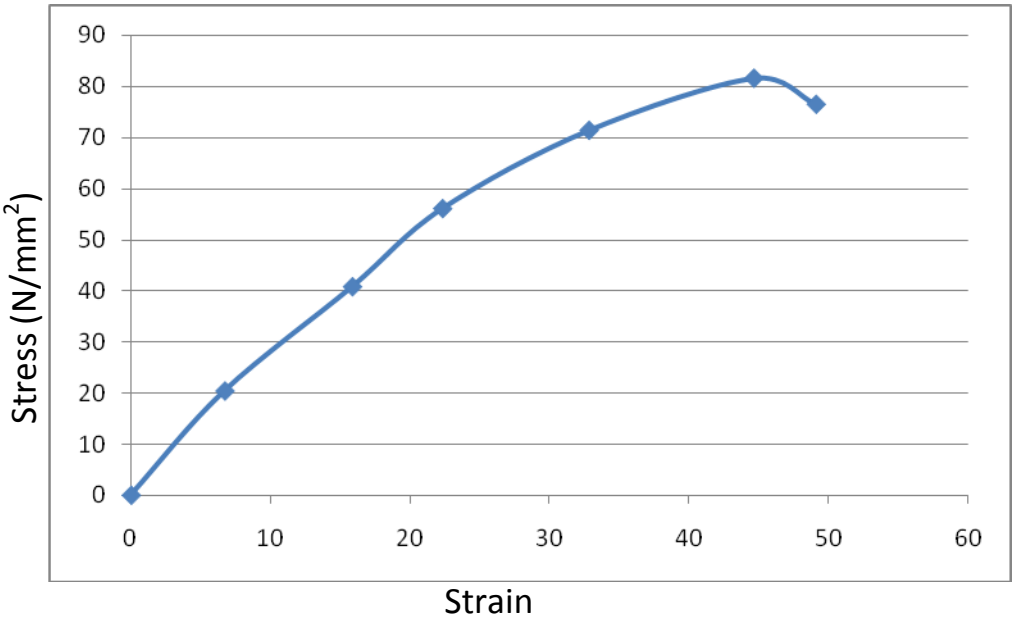

Figure 4.10: Stress-Strain curve for unmodified 30mm x50mm

Table 4.6: Unmodified 40mm x 50mm sample

(N) Load	(mm) Ext.	(mm) L_o	(mm) D_o	(mm) D_f	$(mm)^2$ A_o	(N/mm^2) Stress	$(x1o^{-3})$ Strain	(HRB) Hardness
0	0.000	28	5	4.360	19.642	0.000	0.000	62.500
400	0.238	28	5	4.360	19.642	20.365	8.500	62.500
700	0.494	28	5	4.360	19.642	35.635	17.643	62.500
900	0.625	28	5	4.360	19.642	45.820	22.321	62.500
1500	1.094	28	5	4.360	19.642	76.367	39.071	62.500
1400	1.250	28	5	4.360	19.642	71.276	44.643	62.500
1300	1.406	28	5	4.360	19.642	66.185	50.214	62.500

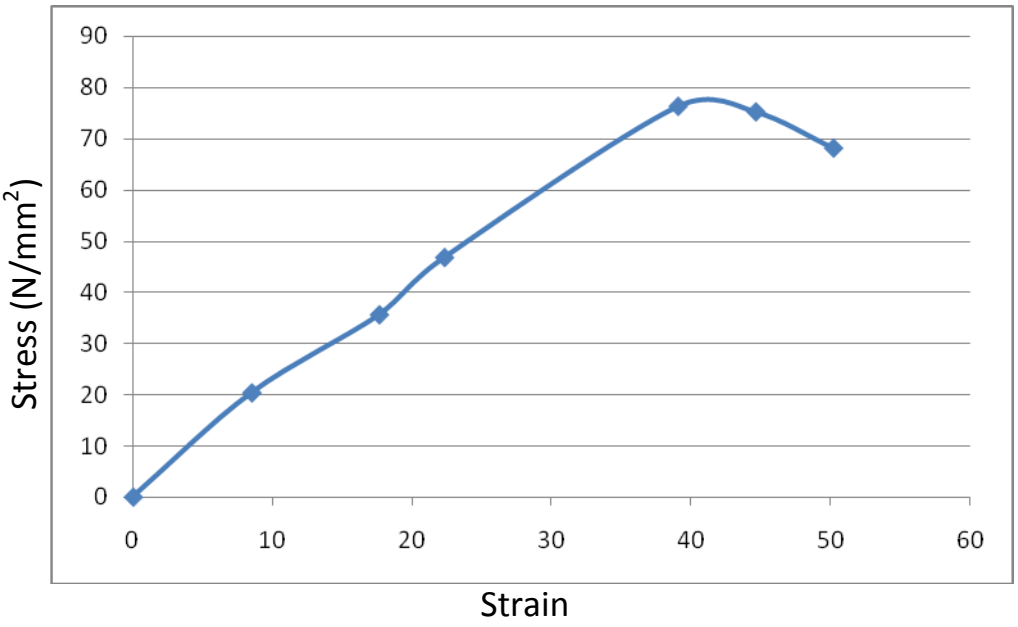

Figure 4.11: Stress-Strain curve for unmodified 40mm x50mm

Plotting the five sections that were not modified in a single plot will further show their differences in tensile strength.

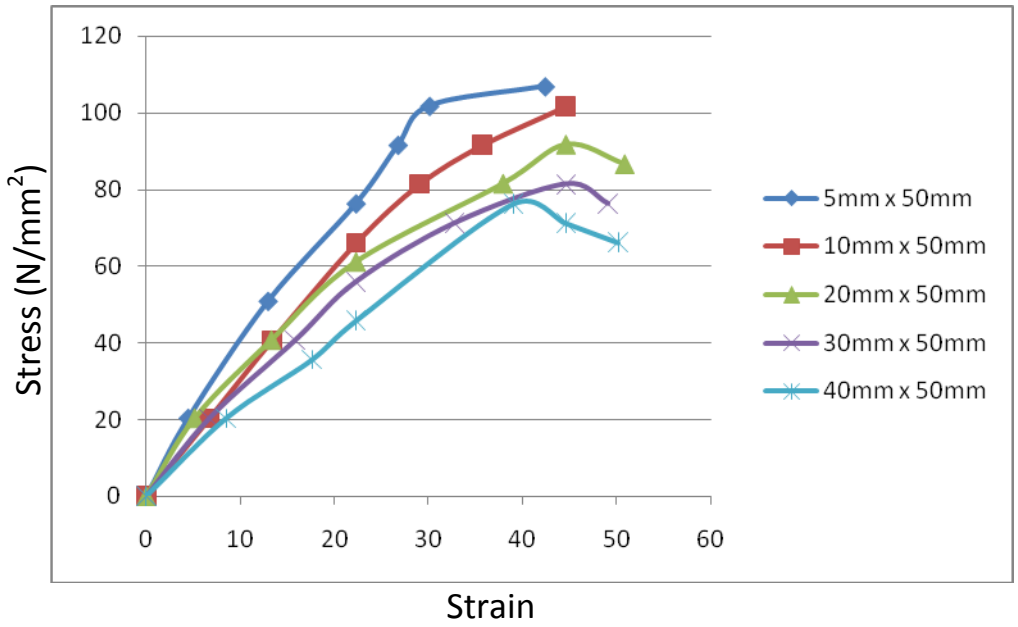

Figure 4.12: combined curves for all the unmodified sections

4.2.2 Sr MODIFIED TEST RESULTS

Table 4.7: Sr modified 5mm x 50mm sample

(N) Load	(mm) Ext.	(mm) L_o	(mm) D_o	(mm) D_f	$(mm)^2$ A_o	(N/mm^2) Stress	$(x1o^{-3})$ Strain	(HRB) Hardness
0	0.000	28	5	4.63	19.642	0.000	0.000	47
400	0.175	28	5	4.63	19.642	20.365	6.250	47
900	0.438	28	5	4.63	19.642	45.825	15.643	47
1300	0.625	28	5	4.63	19.642	66.185	22.321	47
2000	0.938	28	5	4.63	19.642	101.823	30.500	47
2200	1.250	28	5	4.63	19.642	112.005	44.643	47
2100	1.438	28	5	4.63	19.642	106.913	51.358	47

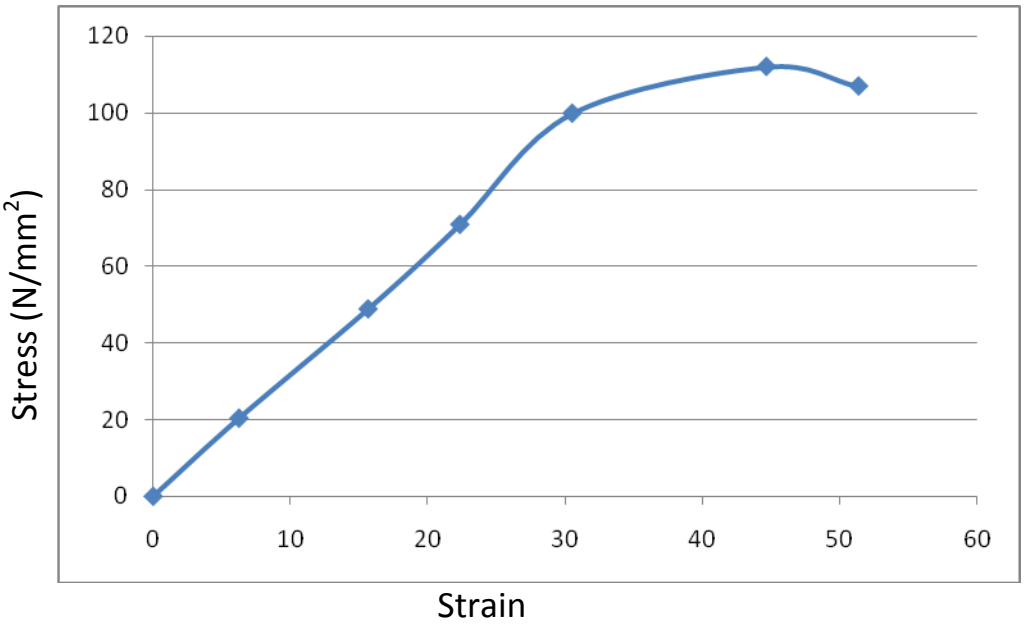

Figure 4.13: Stress-Strain curve for Sr modified 5mm x50mm

Table 4.8: Sr modified 10mm x 50mm sample

(N) Load	(mm) Ext.	(mm) L_o	(mm) D_o	(mm) D_f	$(mm)^2$ A_o	(N/mm^2) Stress	$(x1o^{-3})$ Strain	(HRB) Hardness
0	0.000	28	5	4.58	19.642	0.000	0.000	50
400	0.181	28	5	4.58	19.642	20.365	6.464	50
1000	0.463	28	5	4.58	19.642	50.913	16.536	50
1300	0.625	28	5	4.58	19.642	66.185	22.231	50
1800	0.944	28	5	4.58	19.642	91.640	33.714	50
2000	1.250	28	5	4.58	19.642	101.823	44.643	50
1900	1.444	28	5	4.58	19.642	96.731	51.571	50

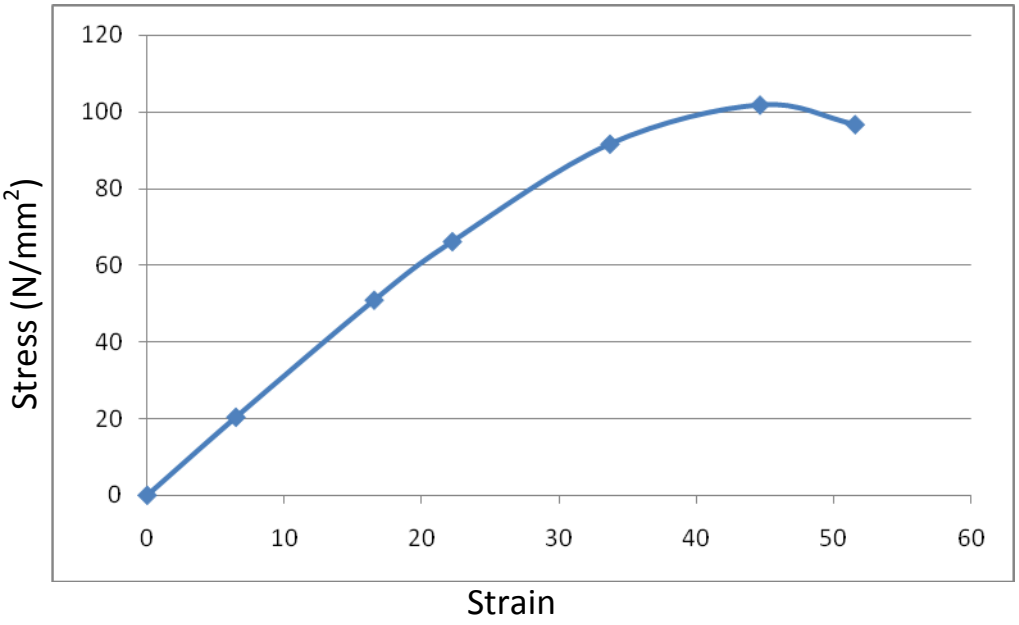

Figure 4.14: Stress-Strain curve for Sr modified 10mm x50mm

Table 4.9: Sr modified 20mm x 50mm sample

(N) Load	(mm) Ext.	(mm) L_o	(mm) D_o	(mm) D_f	$(mm)^2$ A_o	(N/mm^2) Stress	$(x1o^{-3})$ Strain	(HRB) Hardness
0	0.000	28	5	4.47	19.642	0.000	0.000	51
400	0.188	28	5	4.47	19.642	20.365	6.714	51
900	0.469	28	5	4.47	19.642	45.820	16.750	51
1200	0.625	28	5	4.47	19.642	61.094	22.312	51
1600	0.938	28	5	4.47	19.642	81.458	33.500	51
1800	1.313	28	5	4.47	19.642	91.640	46.893	51
1600	1.563	28	5	4.47	19.642	81.458	55.821	51

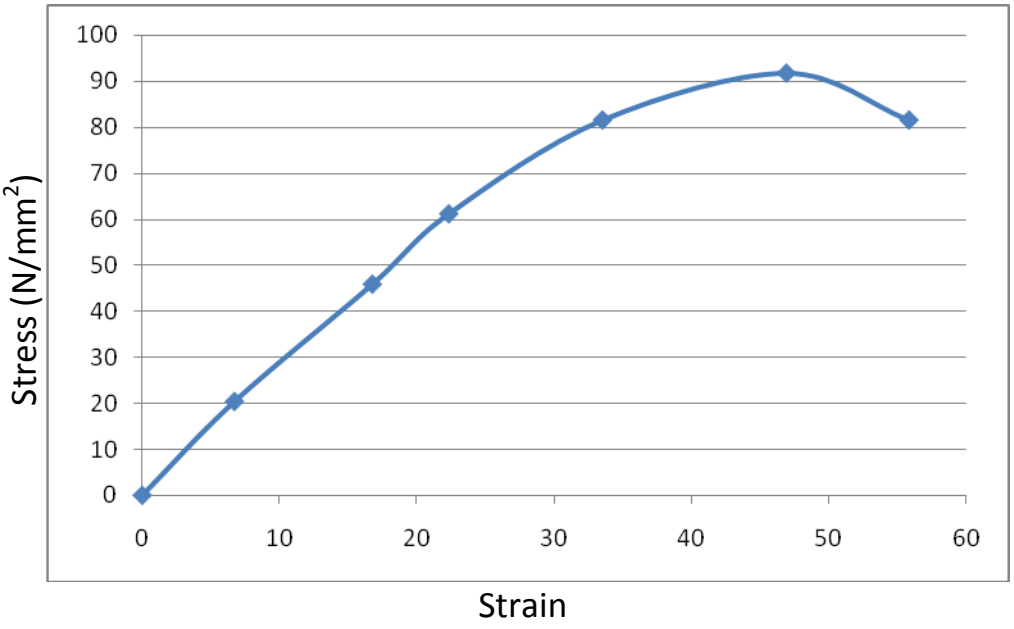

Figure 4.15: Stress-Strain curve for Sr modified 20mm x50mm

Table 4.10: Sr modified 30mm x 50mm sample

(N) Load	(mm) Ext.	(mm) L_o	(mm) D_o	(mm) D_f	$(mm)^2$ A_o	(N/mm^2) Stress	$(x1o^{-3})$ Strain	(HRB) Hardness
0	0.000	28	5	4.32	19.642	0.000	0.000	53.5
600	0.313	28	5	4.32	19.642	30.547	11.179	53.5
1200	0.625	28	5	4.32	19.642	60.094	22.321	53.5
1400	0.938	28	5	4.32	19.642	71.276	33.500	53.5
1600	1.250	28	5	4.32	19.642	81.458	44.643	53.5
1650	1.469	28	5	4.32	19.642	84.004	52.464	53.5
1400	1.719	28	5	4.32	19.642	71.276	61.393	53.5

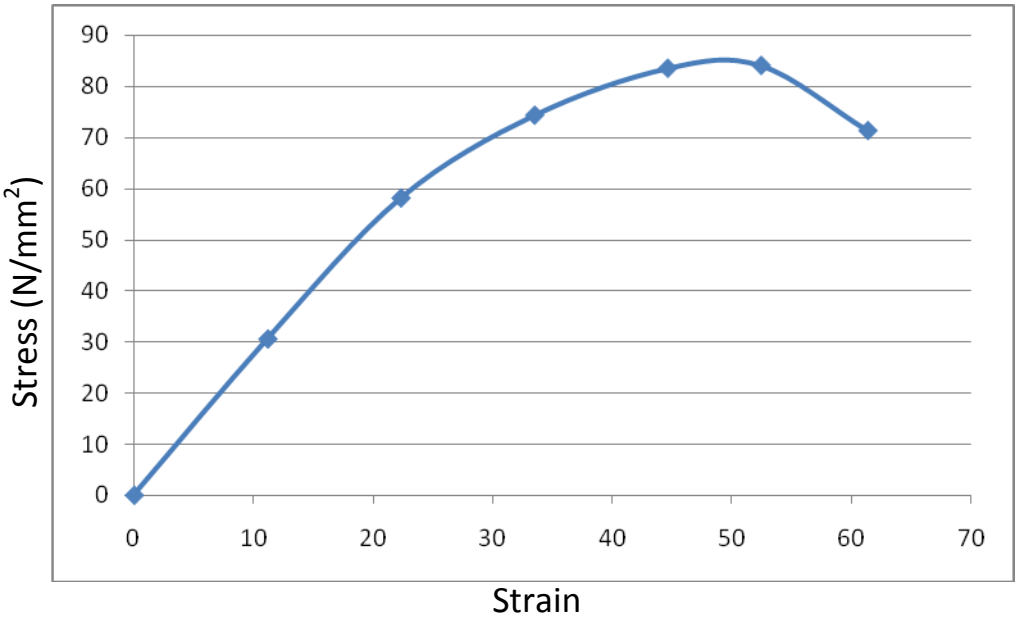

Figure 4.16: Stress-Strain curve for Sr modified 30mm x50mm

Table 4.11: Sr Modified 40mm x 50mm sample

(N) Load	(mm) Ext.	(mm) L_o	(mm) D_o	(mm) D_f	$(mm)^2$ A_o	(N/mm^2) Stress	$(x1o^{-3})$ Strain	(HRB) Hardness
0	0.000	28	5	4.21	19.642	0.000	0.000	55
600	0.313	28	5	4.21	19.642	30.547	11.179	55
1000	0.625	28	5	4.21	19.642	50.911	22.321	55
1300	0.906	28	5	4.21	19.642	66.184	32.357	55
1500	1.250	28	5	4.21	19.642	76.367	44.643	55
1600	1.375	28	5	4.21	19.642	80.458	49.107	55
1300	1.688	28	5	4.21	19.642	66.185	60.286	55

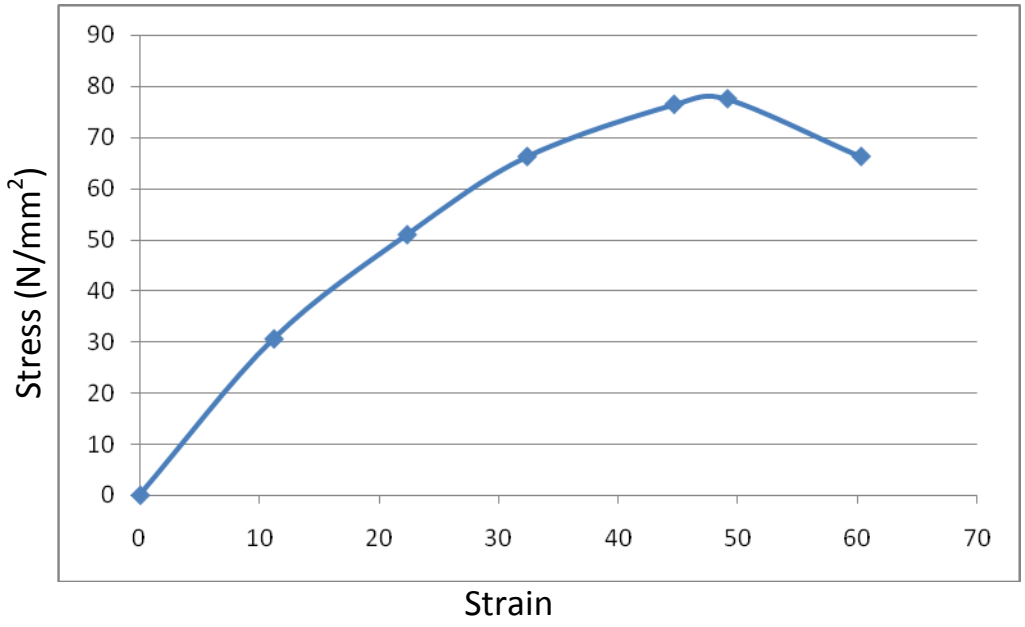

Figure 4.17: Stress-Strain curve for Sr modified 40mm x50m

We can as well plot the stress-strain curve for the Sr modified alloy to see clearer the variation of their strength due to different cooling rates

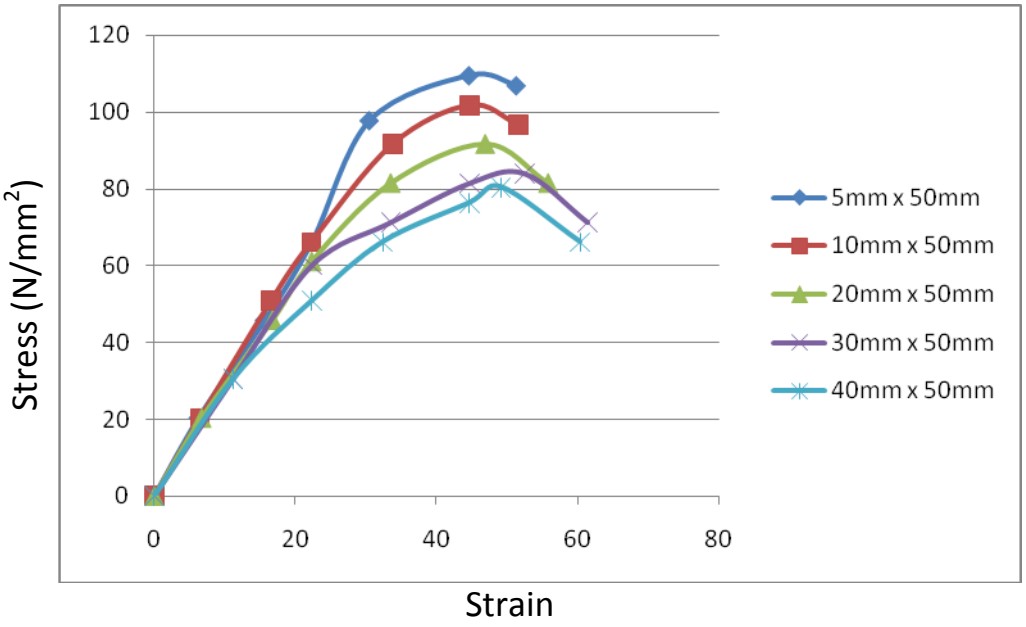

Figure 4.18: Combined curves for all the Sr modified sections

4.2.3 Na MODIFIED TEST RESULT

Table 4.12: Na modified 5mm x 50mm sample

(N) Load	(mm) Ext.	(mm) L_o	(mm) D_o	(mm) D_f	$(mm)^2$ A_o	(N/mm^2) Stress	$(x1o^{-3})$ Strain	(HRB) Hardness
0	0.000	28	5	4.650	19.642	0.000	0.000	46.5
400	0.171	28	5	4.650	19.642	20.365	6.1071	46.5
900	0.420	28	5	4.650	19.642	45.820	15.00	46.5
1300	0.613	28	5	4.650	19.642	66.185	21.890	46.5
2000	0.899	28	5	4.650	19.642	101.832	32.107	46.5
2200	1.231	28	5	4.650	19.642	112.005	43.964	46.5
2100	1.418	28	5	4.650	19.642	106.914	50.643	46.5

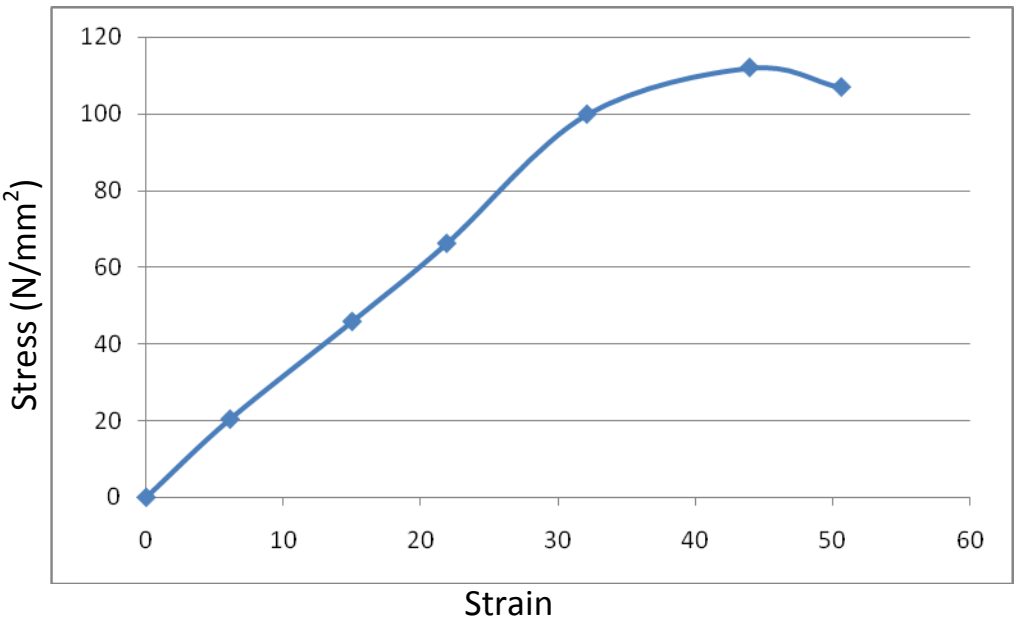

Figure 4.19: Stress-Strain curve for Na modified 5mm x 50mm

Table 4.13: Na modified 10mm x 50mm sample

(N) Load	(mm) Ext.	(mm) L_o	(mm) D_o	(mm) D_f	$(mm)^2$ A_o	(N/mm^2) Stress	$(x1o^{-3})$ Strain	(HRB) Hardness
0	0.000	28	5	4.580	19.642	0.000	0.000	48
400	0.179	28	5	4.580	19.642	20.365	6.393	48
1000	0.460	28	5	4.580	19.642	50.911	16.429	48
1300	0.618	28	5	4.580	19.642	66.185	22.071	48
1800	0.936	28	5	4.580	19.642	91.640	33.429	48
2000	1.248	28	5	4.580	19.642	101.823	44.571	48
1900	1.436	28	5	4.580	19.642	96.731	51.286	48

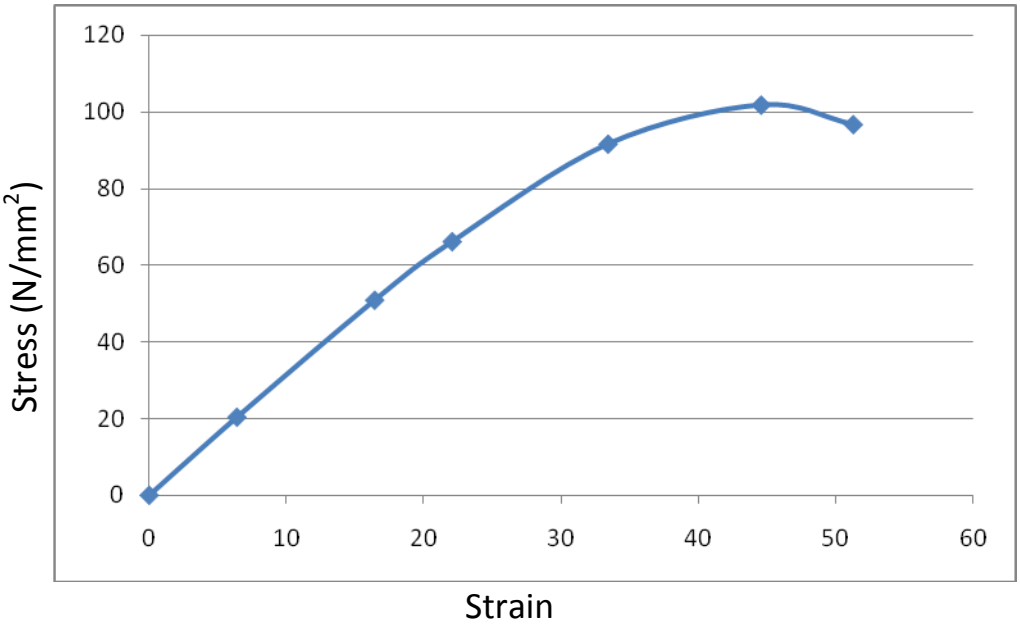

Figure 4.20: Stress-Strain curve for Na modified 10mm x50mm

Table 4.14: Na modified 20mm x 50mm sample

(N) Load	(mm) Ext.	(mm) L_o	(mm) D_o	(mm) D_f	$(mm)^2$ A_o	(N/mm^2) Stress	$(x1o^{-3})$ Strain	(HRB) Hardness
0	0.000	28	5	4.490	19.642	0.000	0.000	50
400	0.184	28	5	4.490	19.642	20.365	6.571	50
900	0.461	28	5	4.490	19.642	45.820	16.464	50
1200	0.622	28	5	4.490	19.642	61.094	22.214	50
1600	0.932	28	5	4.490	19.642	81.450	33.386	50
1800	1.311	28	5	4.490	19.642	91.640	46.821	50
1600	1.560	28	5	4.490	19.642	81.458	55.714	50

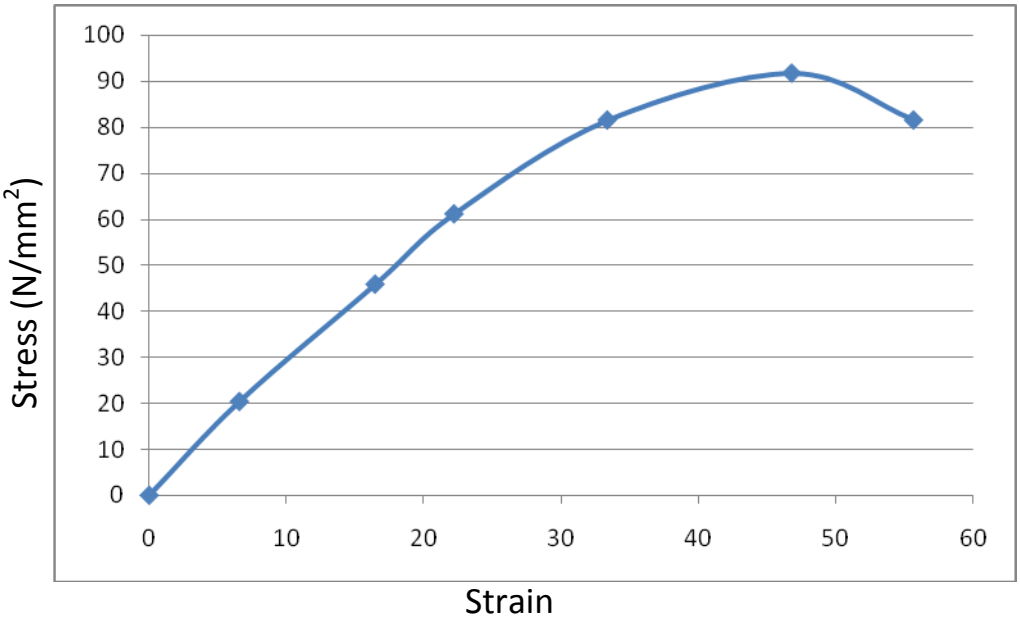

Figure 4.21: Stress-Strain curve for Na modified 20mm x50mm

Table 4.15: Na modified 30mm x 50mm sample

(N) Load	(mm) Ext.	(mm) L_o	(mm) D_o	(mm) D_f	$(mm)^2$ A_o	(N/mm^2) Stress	$(x1o^{-3})$ Strain	(HRB) Hardness
0	0.000	28	5	4.35	19.642	0.000	0.000	
600	0.311	28	5	4.35	19.642	30.547	11.107	
1200	0.620	28	5	4.35	19.642	61.094	22.143	
1400	0.931	28	5	4.35	19.642	71.276	33.250	
1600	1.243	28	5	4.35	19.642	81.458	44.393	
1650	1.463	28	5	4.35	19.642	84.004	52.250	
1400	1.698	28	5	4.35	19.642	71.276	60.643	

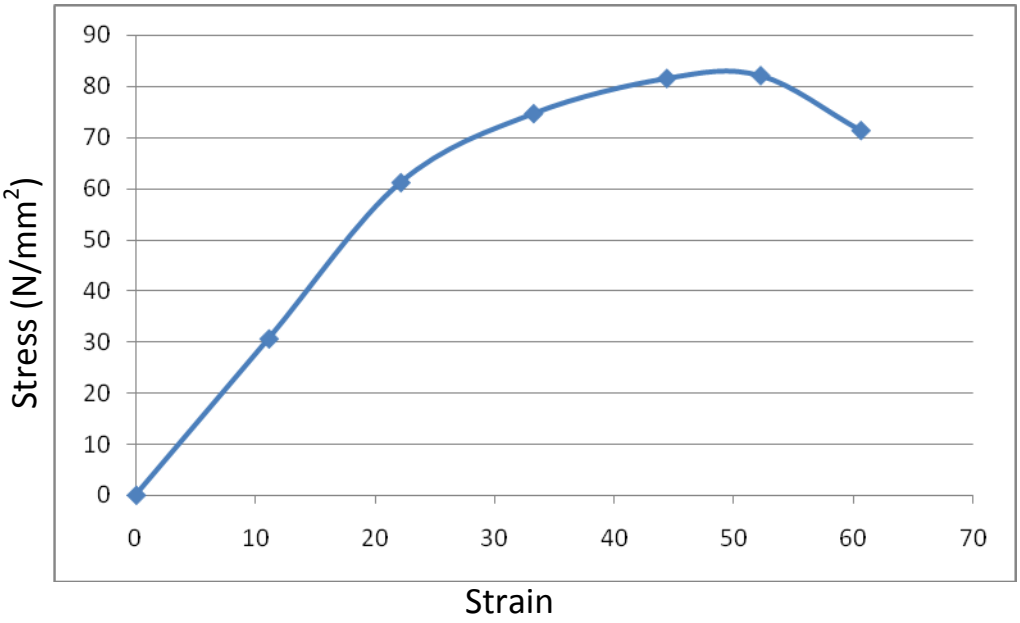

Figure 4.22: Stress-Strain curve for Na modified 30mm x50mm

Table 4.16: Na modified 40mm x 50mm sample

(N) Load	(mm) Ext.	(mm) L_o	(mm) D_o	(mm) D_f	$(mm)^2$ A_o	(N/mm^2) Stress	$(x1o^{-3})$ Strain	(HRB) Hardness
0	0.000	28	5	4.240	19.642	0.000	0.000	53
600	0.301	28	5	4.240	19.642	30.547	10.750	53
100	0.621	28	5	4.240	19.642	50.911	22.179	53
1300	0.900	28	5	4.240	19.642	66.185	32.143	53
1500	1.238	28	5	4.240	19.642	76.367	44.217	53
1600	1.371	28	5	4.240	19.642	81.458	48.964	53
1300	1.682	28	5	4.240	19.642	66.185	60.071	53

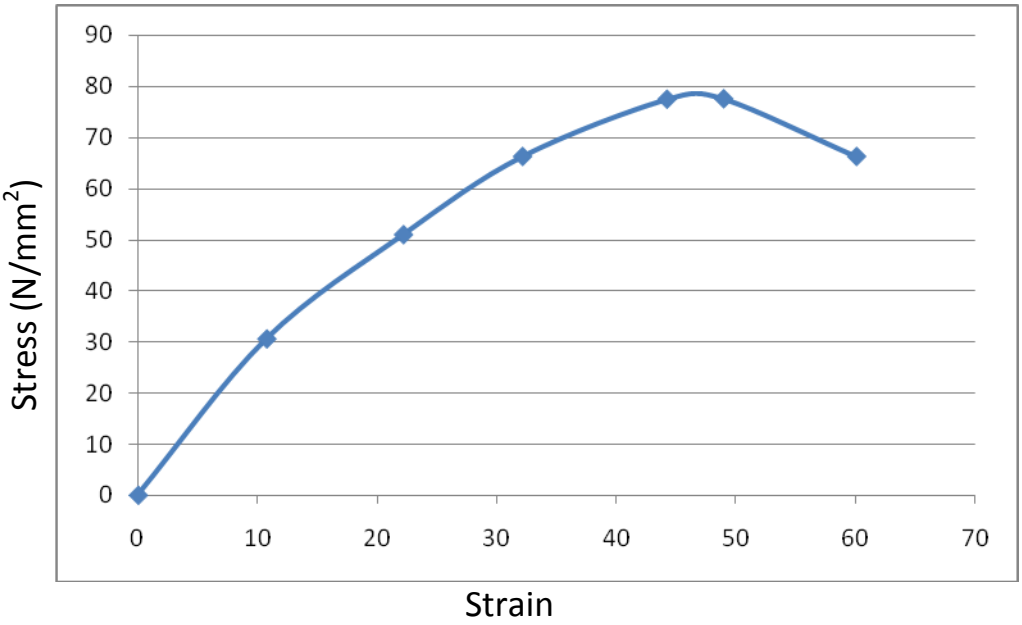

Figure 4.23: Stress-Strain curve for Na modified 40mm x 50mm

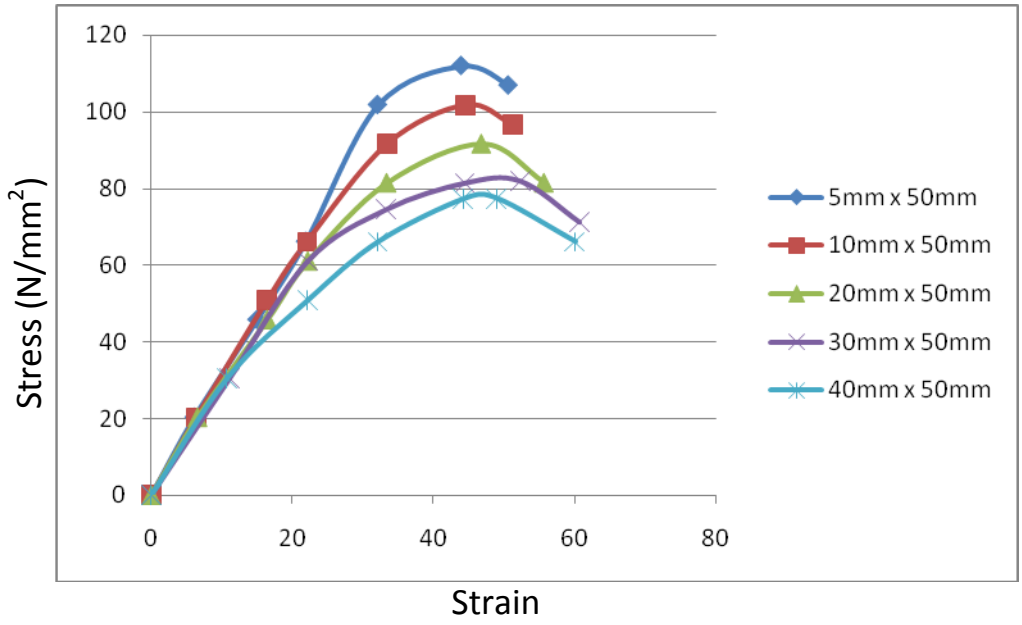

Figure 4.24: Combined curves for all the Na modified sections

From the graphs plotted above, it has been shown that modification has great effect on the tensile properties of the test samples. It was observed that the

castings modified with strontium and sodium have similar effect on the tensile properties of the alloy. The three samples produced are of the same composition except that one was unmodified, one was Sr modified while the other one was Na modified. Sr modified showed slightly better strength and elongation from their stress strain curves.

From this research, one can go further to reveal the effect of cooling rate and modifications on the hardness properties of the samples produced. It was discovered that fast cooling rates have better hardness than slow cooling rates. Sections with small thicknesses have high cooling rates while those with bigger thickness have slow cooling rates and as a result the small section castings resisted Rockwell Hardness test better than the big section castings. This explains the reason the samples with faster cooling rates have smaller indentations on their surfaces during hardness test. The samples with slower cooling rates have deeper indentation as can be seen from the hardness values in the tables above. This is indicative that the hardness of a material increases with decreasing solidification time during material processing. The Rockwell hardness values for the different sections in the three samples are tabulated among the tensile properties data in the above tables.

4.3 MICROSTRUCTURES

The results obtained from the microstructural analyses significantly revealed the effect of cooling rate on the microstructure of Al-Si-Mg alloy. It has a noticeable effect of different cooling rate due to difference in thickness of the test samples. The structure of cast Al-Si-Mg alloy consists of the α-Al solid solution which is the matrix and some intermetallic secondary phases, β-Si in the form of large flakes, needle like and fibrous precipitates. We also have Al_2Mg eutectic since Mg and Si are the major alloying elements used.

It is evident that the cooling rates have influence on the grain size. It has been established here that cooling rates can be used to control grain sizes. Fast cooling rate gives fine grain structures while slow cooling rates produce coarse grain structures. Figures of micrographs below in this section show the variation of the grain size and secondary dendrite arm spacing (SDAS) as a function of cooling rates. It can be seen from the structures that increase in cooling rate decreases the grain size and SDAS. Micrograph of each section has different structure as a result of change in cooling rate this also confirms the reduction of SDAS. Sections with slow cooling rate have bigger DSAS while sections with fast cooling rates have smaller SDAS and hence small grained structures. We have also seen that the size of silicon particles in this alloy is dependent on the solidification time. In this investigated alloy, the increase in solidification rate results in significant reduction of Si particle size.

Modifications with strontium and sodium have effect on the Si particle morphology. Also the cooling rate has effect on the percentage of silicon modification level (SML). The trend here indicates that an increase in solidification rate significantly increase the percentage of SML. The eutectic silicon crystals can change from large flakes into a fibrous structure (globular) that can be further modified to fine grained structures.

In the microstructures below, it is evident that not all the silicon particles that were modified. The structures show needle-like and globular silicon particles indicative of presence of both lamellar and fibrous structures coexisting together. As the cooling rates increased from the bigger section (40mm x 50mm) to the smallest section (5mm x 50mm), silicon morphology modification improves for both Sr and Na modified. This modification of the grain's SDAS is good for the alloy as it improves the quality of the alloy.

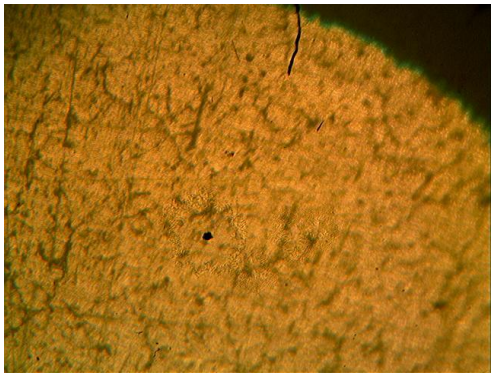
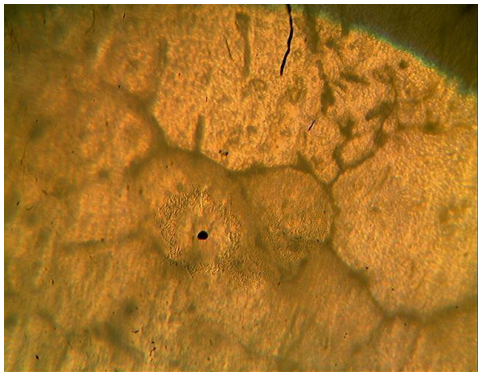

X100 X400

Plate 4.1: Microstructures of unmodified alloy (5mm x 50mm)

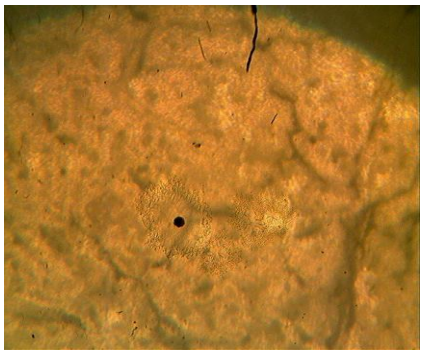
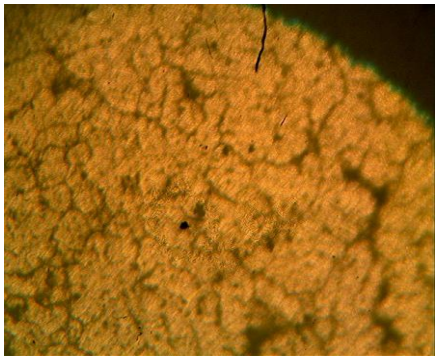

X100 X400

Plate 4.2: Microstructures of unmodified alloy (10mm x 50mm)

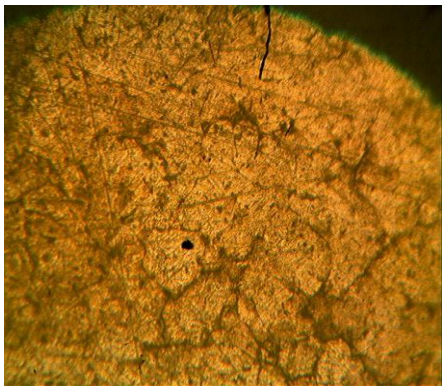
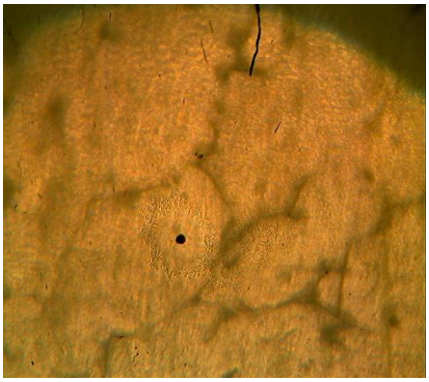

X100 X400

Plate 4.3: Microstructures of unmodified alloy (20mm x 50mm)

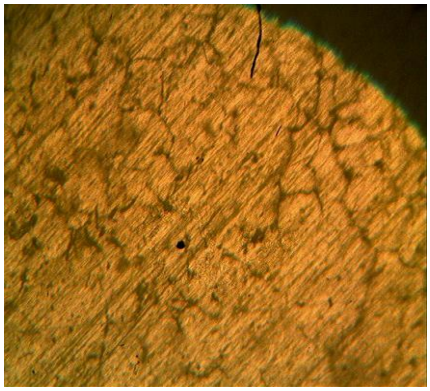

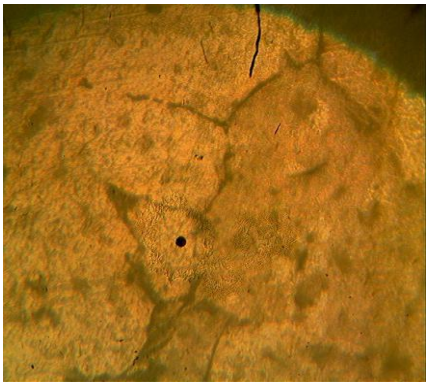

X100 X400

Plate 4.4: Microstructures of unmodified alloy (30mm x 50mm)

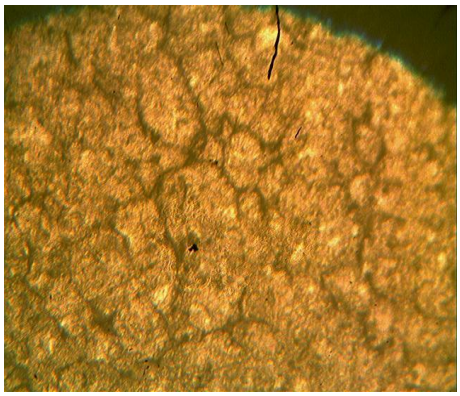

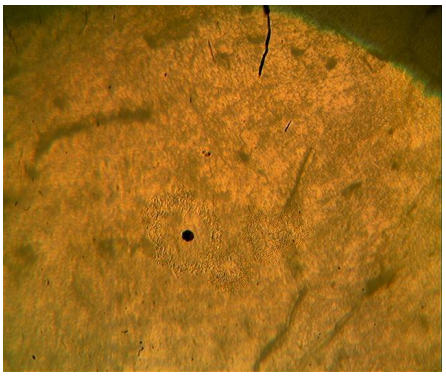

X100 400

Plate 4.5: Microstructures of unmodified alloy (40mm x 50mm)

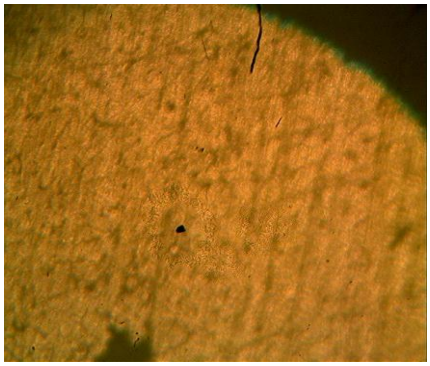

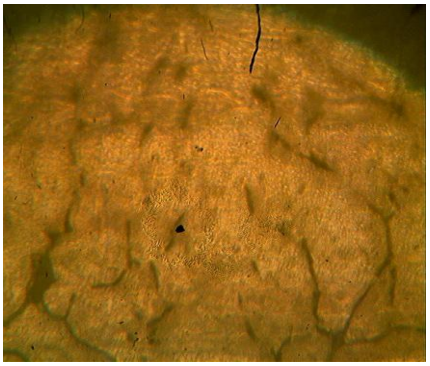

X100 X400

Plate 4.6: Microstructures of Sr modified alloy (5mm x 50mm)

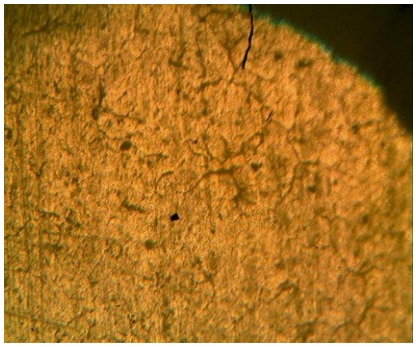

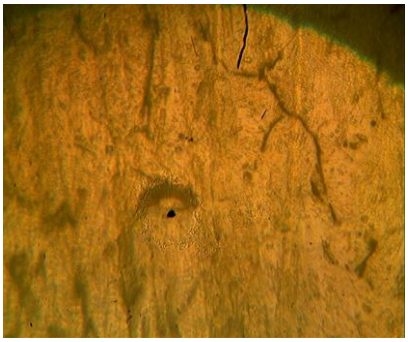

X100 X400

Plate 4.7: Microstructures of Sr modified alloy (10mm x 50mm)

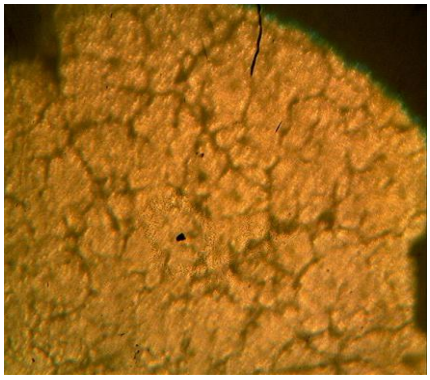

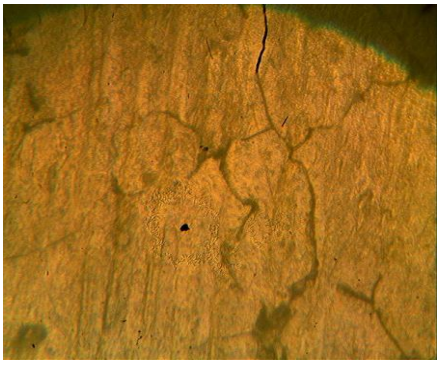

X100 X400

Plate 4.8: Microstructures of Sr modified alloy (20mm x 50mm)

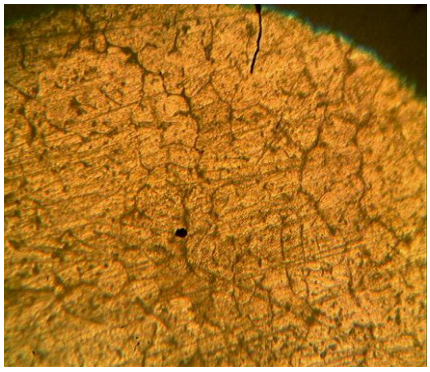

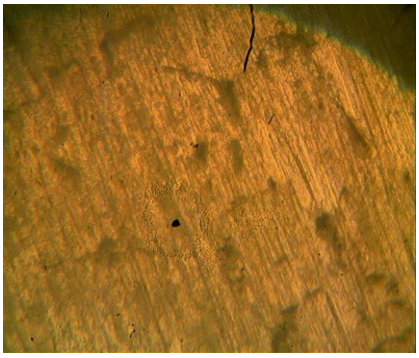

X100 X400

Plate 4.9: Microstructures of Sr modified alloy (30mm x 50mm)

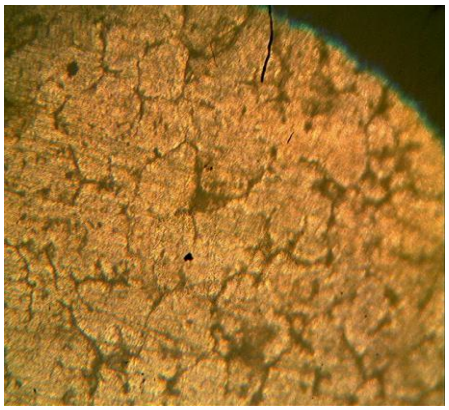

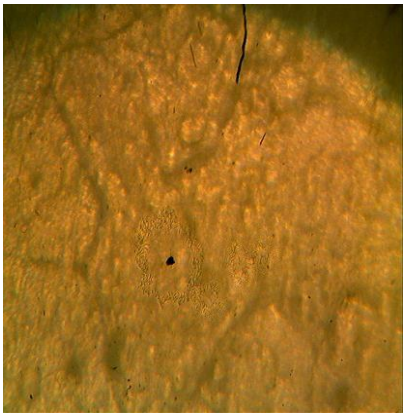

X100 X400

Plate 4.10: Microstructures of Sr modified alloy (40mm x 50mm)

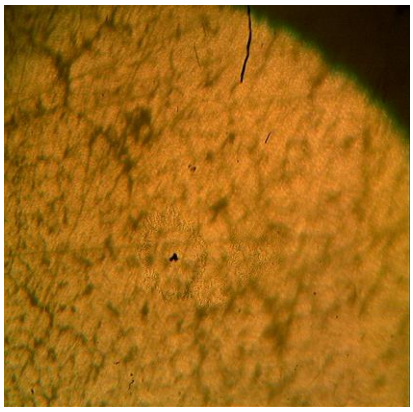

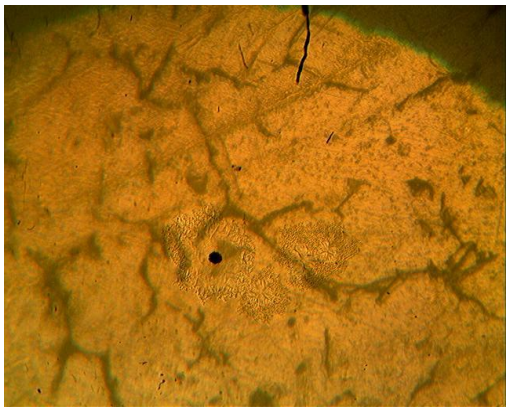

X100 X400

Plate 4.11: Microstructures of Na modified alloy (5mm x 50mm)

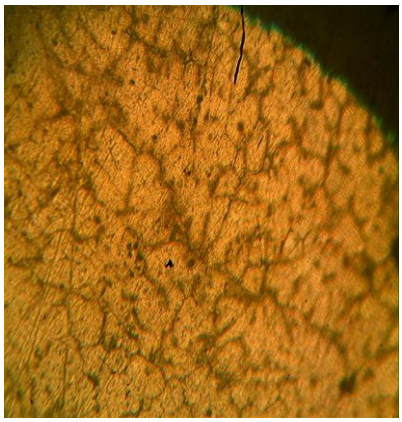

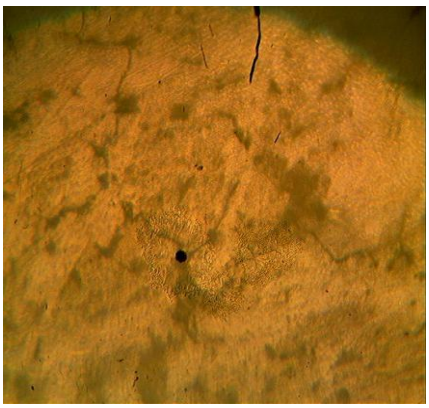

X100 X400

Plate 4.12: Microstructures of Na modified alloy (10mm x 50mm)

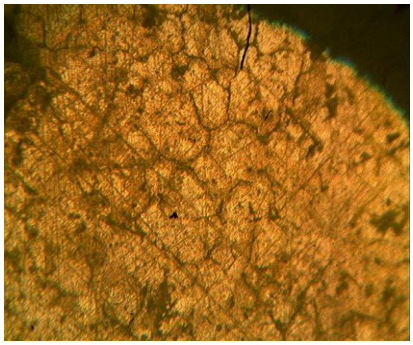

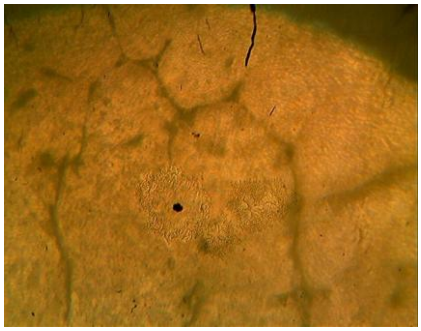

X100 X400

Plate 4.13: Microstructures of Na modified alloy (20mm x 50mm)

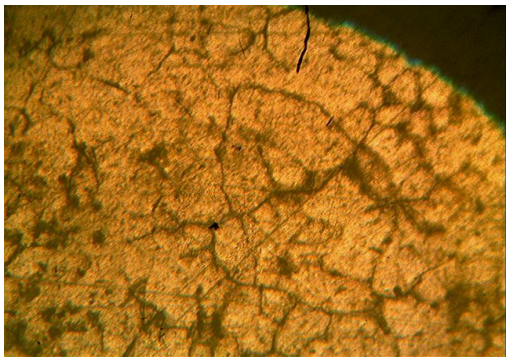

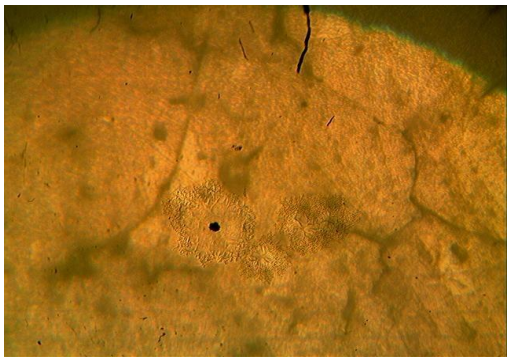

X100 X400

Plate 4.14: Microstructures of Na modified alloy (30mm x 50mm)

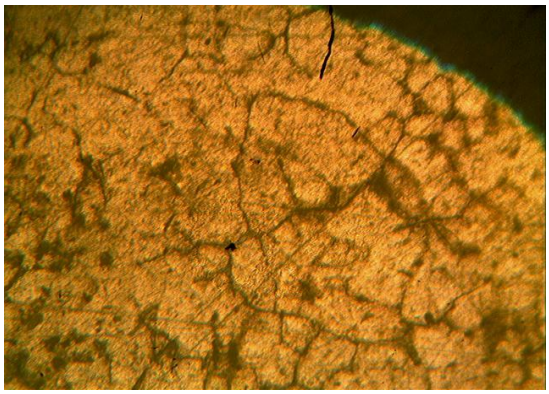

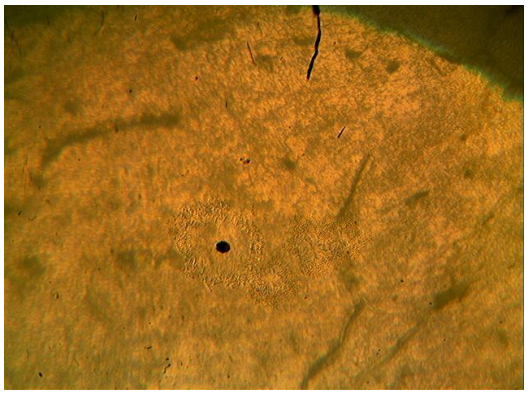

X100 X400

Plate 4.15: Microstructures of Na modified alloy (40mm x 50mm)

CHAPTER FIVE

CONCLUSIONS AND RECOMMENDATIONS

5.1 CONCLUSIONS

The effect of cooling rate and modification on the microstructure and tensile properties of Al-Si-Mg alloy such as tensile strength, hardness, grain size, was observed. The results can be summarised as follows

1. The difference in cooling rates was due to difference in section thickness of the pattern used. Since a single mould was used, heat diffusivity cannot be used to explain the variation in cooling rates.
2. From the cooling rate curves in section 4.1, it was observed that solidification parameters such as solidification range and solidification time are affected by cooling rate. The formation temperatures of various phases are changed with an increasing cooling rate.
3. Increasing the cooling rate increases the Aluminium nucleation temperature and reduces nucleation time. This also increases nucleation undercooling temperature and decreases the undercooling temperature. It leads to an increased number of nuclei that also affect the grain size and secondary dendrite arm spacing.
4. The cooling rates have been found to impact significantly on the mechanical properties such as UTS, ductility, hardness etc. This is revealed in the stress – strain curves plotted in section 4.2.
5. The structures that were modified with strontium and sodium have better structural and mechanical properties due to the change of morphologies of their silicon particles.

5.2 RECOMMENDATION

From the findings made in this research work, it has been observed that cooling rates have great effect on the tensile properties and microstructure of Al-Si-Mg alloy. It is therefore strongly recommended that alloy's design and process engineers have a wide range of solidification rates to choose from i.e process parameters.

It is also recommended to them to modify alloys with modifiers that will best suit the service conditions of the particular system. For example, it should be recommended that Na between Na and Sr if hardness is desired since the structures that are Na modified resisted Rockwell hardness tester indentation better than the Sr modified structures.

REFERENCES

Abbaschain, R. And Ravitz S.F, Crystal growth 28, (1975) 16.

Abbaschian and Kurz W. In Solidification processes and microstructures, TMS Publications, 2004, p. 319-324.

Books C.R, Heat Treatment, Structure and Properties of non-Ferrous Alloys, ASM, Metals Park, Ohio, USA, 1982, P. 79-82.

Campbell J. Castings, Butterworth-Heineman Ltd, Oxford, England, 1991, p.146.

Campbell J. Castings, Butterworth-Heinemann Ltd Oxford, England, 1991, p.143.

Campbell J. Castings, Butterworth-Heinemann Ltd, Oxford, England, 1991, p. 285.

Clyne T.W, Kurz W, Metallugical Transactions 12A (1981) 965.

Cole G.S, In Solidification, American Society for Metals, Metals Park, Ohio, 1971.

Flemings M.C, Scandinavian Journal of Metallurgy 51 (1976) 1.

Geiger G.H, Poirier D.R, Transport Phenomena in Metallurgy Addison Welsley, 1973.

Grusleski J.E, Closset M.B, Mulazimogbu H, Tenekedjeu N. Thermal analysis of Strontium-Treated Aluminium Alloys, Afs, Des Plaines, Illonois 1974, p.283.

Gruzleski J.E, Microstructure Development during Casting, Afs, Des Plaines, Illinois, USA, 2000, p. 112-113.

Hansen P.N, In Solidification and casting of metals, The Metal Society, London, 1979.

Kammar I.C, Aluminium Handbook, Aluminium-Verlay, Dusseldorf, Germany, 1999, p. 86.

Kirwood D.H, Evans D.J, In the Solidification of Metals, Iron and Steel Institute, London, Publication 110, 1968.

Kotzin E.L, Metal Casting and Moulding Process, Afs, Des Plaines Illinois, USA, 1992, p. 149-153

Kudo K, and Pehike R.D, Thermal Propertises of moulding Sands, Asf Transactions, vol. 93, 1985, p.405-414

Kurz W, Giovanola B. and Trivedi R. Journal of Crystal growth 91 (1988) 123.

Kurz W. and Fisher D.J, Fundamentals of Solidification, Trans Tech Publications, 1989, Switzerland.

Lipton J, Kurz W, Trivedi R, Acta Metallurgica 35 (1937) 957

Lu S.Z, Hellawell A. The Changing Mechanism of the Silicon Morphology in Al-Si-Mg modified alloys, Metallurgical Transaction A, Vol. 18a, October 1987, p. 1721-1733

Mehrabian R, Flemings M.C, Metallurgical Transactions 1 (1970) 455.

Okorafor O.E and Loper C.R, Jr, Metallurgical factors affecting the microstructure of expandable polystyrene pattern cast Al-4.25% Cu-1.03 Si Alloy, Asf Transaction, Des Plaines, Illinois, USA, Vol. 90, p.285-295.

Okorafor O.E and Thermal Aspect of Gasifiable pattern moulds and solidification of Al-4.25% Cu-1.03% Si Alloy Casting, Aluminium, No. 62, 1986, p. 110-112.

Pfam W.G, Zone Melting, 2nd Edition, Wiley, New York, 1966.

Poirier D.R, Poirier E.J, Heat Transfer Fundamentals for Metal Casting, TMS, Warrendule, Pennslylania USA, 1994, p. 1-6

Poter D.A, Esterling K.E, phase Transformations in Metals and alloys, Van Nostrand Reinhold Co. Ltd, United Kingdom, 1981, 266.

R.W Monroe, Expandable Pattern Casting, Afs Des Plaines, Illinois, USA, 1992, pp 96-97.

Rao P.N, Manufacturing Technology, foundry, Forming and Welding, Tata McGraw-Hill publishing company, new Delhi, India, 1992, p. 137-141.

Sarreal J. and Abbaschian R, Metallurgical Transactions A, 17a, (1986) 2036.

Singh S.N, Bardes B.P, Flemings M.C, Metallurgical Transactions 1 (1970) 1383.

Weinberg F, Chambers B. Canadian Journal of Physics, 17a, (1951) 382.